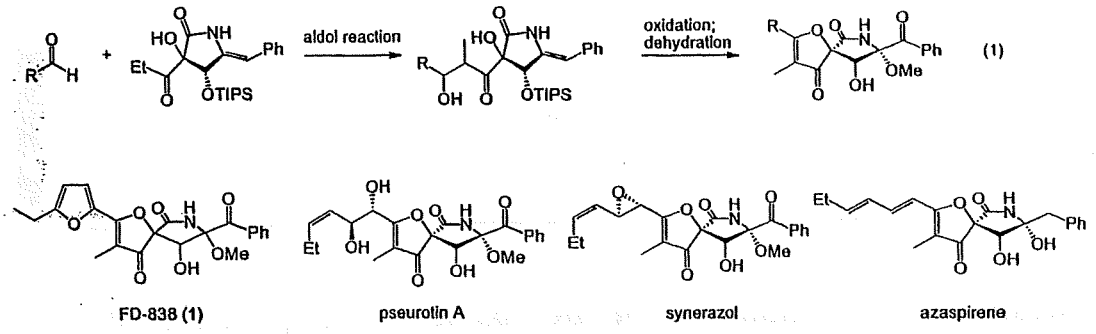

Figure 1. FD-838 (**1**), pseurotin A, synerazol, and azaspirene.

derivatives is required for such biological studies. Because we had established a synthetic method for the latter three natural products, we began to investigate the total synthesis of FD-838. In this communication we report the first total synthesis of FD-838 along with the determination of its absolute configuration.

Because we have already established the synthesis of the azaspirocyclic framework, the same synthetic strategy would be applicable to the synthesis of FD-838. The aldol reaction between 5-ethyl-2-formylfuran and the functionalized benzylidene lactam **2**, which was a key intermediate for other azaspiro compounds prepared from methyl pentenoate via Sharpless dihydroxylation as a key step, was examined.[6–8] The lithium enolate of **2** reacted with 5-ethyl-2-formylfuran, affording the desired aldol product **3** (mixture of four diastereomers, 1:1:3:3.5) in 40% yield with recovery of the lactam **2** in 49% yield (78% yield based on the recovered starting material (br sm)). Oxidation of the alcohol **3** with Dess–Martin periodinane (DMP)[13] in CH_2Cl_2 in the presence of $NaHCO_3$ afforded the 1,3-diketone **5**. When 1,3-diketone **5** was treated with silica gel on TLC, cyclization followed by dehydration proceeded because of the acidity of the silica gel to produce azaspiro derivative **4** in 20% yield with recovery of 1,3-diketone **5** in 37% yield over two steps. Recovered 1,3-diketone **5** was further transformed into azaspiro derivative **4** in 27% yield (54% br sm) by the same reaction conditions. Oxidation of the benzylidene moiety with dimethyldioxirane (DMD)[14] in MeOH afforded a mixture of methoxy derivative **6** and hydroxy derivative **7** in 56% yield (single diastereomers at the benzylic alcohol position), the mixture of which was treated with DMP in CH_2Cl_2 to provide benzoylated methoxy **8** and hydroxy **9** derivatives in 49% and 16% yields, respectively, which can be separated by TLC. Removal of the TIPS group with NH_4F in MeOH afforded FD-838 (**1**) in 62% yield (89%, br sm). Synthetic FD-838 exhibited identical properties to those of the natural substance (^1H NMR, ^{13}C NMR, IR).

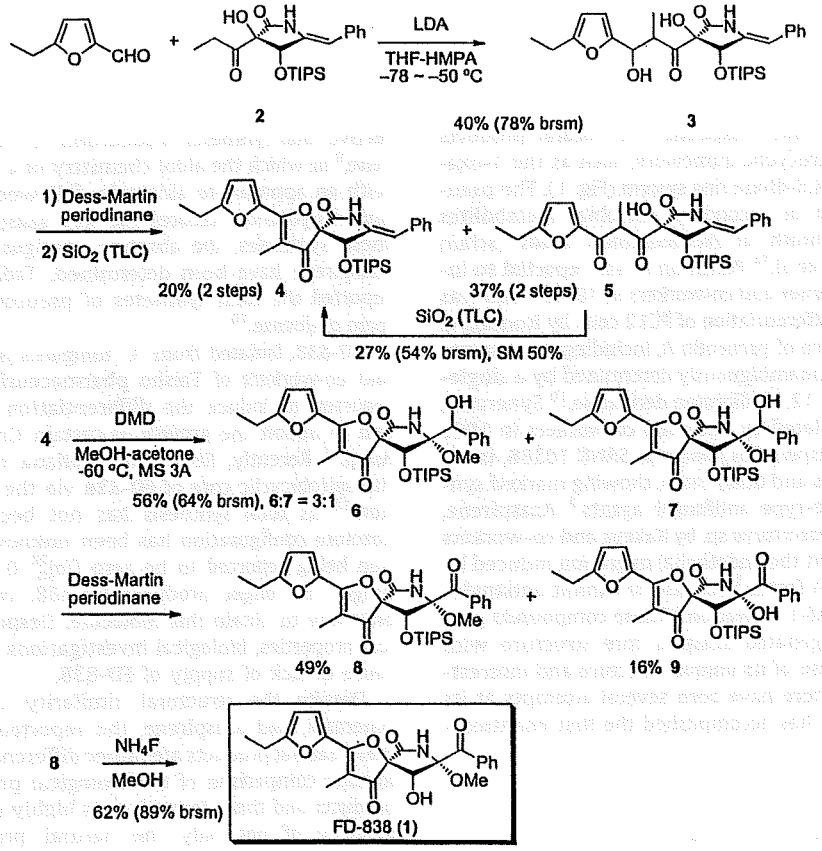

Scheme 1. The synthesis of FD-838.

Because the optical rotation of natural FD-838 was reported to be zero using MeOH as a solvent,[11] the optical rotation was measured in other solvents, such as $CHCl_3$. The optical rotations of natural FD-838 and synthetic FD-838 show large negative values (synthetic FD-838: $[\alpha]_D^{26}$ −41.9 (*c* 0.4, $CHCl_3$), natural FD-838: $[\alpha]_D^{26}$ −32.4 (*c* 0.7, $CHCl_3$)), indicating that both compounds have the same absolute configuration.[15] Thus, the absolute configuration is determined, as shown in Scheme 1.

In summary, we have accomplished the first asymmetric total synthesis of FD-838 along with the determination of its absolute configuration.

Acknowledgment

This work was supported by a Grant-in Aid for Scientific Research from the Ministry of Education, Culture, Sports, Science and Technology, Government of Japan.

Supplementary data

Supplementary data associated with this article can be found, in the online version, at doi:10.1016/j.bmcl.2009.03.154.

References and notes

1. (a) Bloch, P.; Tamm, C.; Bollinger, P.; Petcher, T. J.; Weber, H. P. *Helv. Chim. Acta* **1976**, *59*, 133; (b) Weber, H. P.; Petcher, T. J.; Bloch, P.; Tamm, C. *Helv. Chim. Acta* **1976**, *59*, 137; (c) Bloch, P.; Tamm, C. *Helv. Chim. Acta* **1981**, *64*, 304; (d) Breitenstein, W.; Chexal, K. K.; Mohr, P.; Tamm, C. *Helv. Chim. Acta* **1981**, *64*, 379; (e) Wenke, J.; Anke, H.; Sterner, O. *Biosci., Biotechnol., Biochem.* **1993**, *57*, 961; (f) Komagata, D.; Fujita, S.; Yamashita, N.; Saito, S.; Morino, T. *J. Antibiot.* **1996**, *49*, 958.
2. Ando, O.; Satake, H.; Nakajina, M.; Sato, A.; Nakamura, T.; Kinoshita, T.; Furuya, K.; Haneishi, T. *J. Antibiot.* **1991**, *44*, 382.
3. Asami, Y.; Kakeya, H.; Onose, R.; Yoshida, A.; Matsuzaki, H.; Osada, H. *Org. Lett.* **2002**, *4*, 2845.
4. Asami, Y.; Kakeya, H.; Komi, Y.; Kojima, S.; Nishikawa, K.; Beebe, K.; Neckers, L.; Osada, H. *Cancer Sci.* **2008**, *99*, 1853.
5. Synthetic studies of pseurotin A; see: (a) Dolder, M.; Shao, X.; Tamm, C. *Helv. Chim. Acta* **1990**, *73*, 63; (b) Shao, X.; Dolder, M.; Tamm, C. *Helv. Chim. Acta* **1990**, *73*, 483; (c) Su, Z.; Tamm, C. *Helv. Chim. Acta* **1995**, *78*, 1278; (d) Su, Z.; Tamm, C. *Tetrahedron* **1995**, *51*, 11177; (e) Mitchell, J. M.; Finney, N. S. *Org. Biomol. Chem.* **2005**, *3*, 4274; Biosynthetic study, see: (f) Igarashi, Y.; Yabuta, Y.; Sekine, A.; Fujii, K.; Harada, K.; Oikawa, T.; Sato, M.; Furumai, T.; Oki, T. *J. Antibiot.* **2004**, *57*, 748.
6. Hayashi, Y.; Shoji, M.; Yamaguchi, S.; Mukaiyama, T.; Yamaguchi, J.; Kakeya, H.; Osada, H. *Org. Lett.* **2003**, *5*, 2287.
7. Hayashi, Y.; Shoji, M.; Mukaiyama, T.; Gotoh, H.; Yamaguchi, S.; Nakata, M.; Kakeya, H.; Osada, H. *J. Org. Chem.* **2005**, *70*, 5643.
8. Hayashi, Y.; Shoji, M.; Yamaguchi, J.; Sato, K.; Yamaguchi, S.; Mukaiyama, T.; Sakai, K.; Asami, Y.; Kakeya, H.; Osada, H. *J. Am. Chem. Soc.* **2002**, *124*, 12078.
9. Igarashi and co-workers also determined the absolute configuration of synerazol using modified MTPA method, see: Igarashi, Y.; Yabuta, Y.; Furumai, T. *J. Antibiot.* **2004**, *57*, 537.
10. (a) Aoki, S.; Ohi, T.; Shimizu, K.; Shiraki, R.; Takao, K.; Tadano, K. *Heterocycles* **2004**, *62*, 161; (b) Aoki, S.; Ohi, T.; Shimizu, K.; Shiraki, R.; Takao, K.; Tadano, K. *Bull. Chem. Soc. Jpn.* **2004**, *77*, 1703; Review, see: (c) Takao, K.; Aoki, S.; Tadano, K. *J. Syn. Org. Chem. Jpn.* **2007**, *65*, 460.
11. Mizoue, K.; Okazaki, T.; Hanada, K.; Amamoto, T.; Yamagishi, M.; Omura, S. Eur. Pat. Appl. EP 216607, J P Appl. 205278; *Chem. Abstr.*, **1987**, *107*, 132627x.
12. Orellana, A.; Rovis, T. *Chem. Commun.* **2008**, 730.
13. (a) Dess, D. B.; Martin, J. C. *J. Org. Chem.* **1983**, *48*, 4155; (b) Dess, D. B.; Martin, J. C. *J. Am. Chem. Soc.* **1991**, *113*, 7277; (c) Ireland, R. E.; Liu, L. *J. Org. Chem.* **1993**, *58*, 2899; (d) Meyer, S. D.; Schreiber, S. L. *J. Org. Chem.* **1994**, *59*, 7549.
14. (a) Adam, W.; Bialas, J.; Hadjiarapoglou, L. *Chem. Ber.* **1991**, *124*, 2377; (b) Koseki, Y.; Kusano, S.; Ichi, D.; Yoshida, K.; Nagasaka, T. *Tetrahedron* **2000**, *56*, 8855.
15. A small quantity of the natural FD-838 would cause the inconsistency of the optical rotation.

CHEMBIOCHEM

DOI: 10.1002/cbic.200800787

Identification of Cytochrome P450s Required for Fumitremorgin Biosynthesis in *Aspergillus fumigatus*

Naoki Kato,[a] Hirokazu Suzuki,[a, d] Hiroshi Takagi,[a] Yukihiro Asami,[a, e] Hideaki Kakeya,[a, f] Masakazu Uramoto,[a] Takeo Usui,[b] Shunji Takahashi,[a] Yoshikazu Sugimoto,[c] and Hiroyuki Osada*[a]

Fumitremorgin C, a diketopiperazine mycotoxin produced by *Aspergillus fumigatus*, is a potent and specific inhibitor of breast cancer resistance protein (BCRP). Elucidation of the fumitremorgin C biosynthetic pathway provides a strategy for new drug design. A structure–activity relationship study based on metabolites related to the *ftm* gene cluster revealed that the process most crucial for inhibitory activity against BCRP was cyclization to form fumitremorgin C. To determine the gene involved in the cyclization reaction, targeted gene inactivation was performed with candidate genes in the *ftm* cluster. Analysis of the gene disruptants allowed us to identify *ftmE*, one of the cytochrome P450 genes in the cluster, as the gene responsible for the key step in fumitremorgin biosynthesis. Additionally, we demonstrated that the other two cytochrome P450 genes, *ftmC* and *ftmG*, were involved in hydroxylation of the indole ring and successive hydroxylation of fumitremorgin C, respectively.

Introduction

Breast cancer resistance protein (BCRP) is a member of the multidrug transporters of the ATP-binding cassette family, which can actively extrude a wide range of structurally diverse drugs, toxins, endogenous compounds, and their metabolites across the plasma membranes of cells.[1,2] Although these ATP-dependent efflux pumps were once thought to be of relevance only to multidrug resistance in cancer cells, it is now clear that they have a pronounced role in the pharmacokinetics of a broad range of drugs and toxins. It is noteworthy that recent findings have revealed intriguing roles for BCRP in stem cells.[2,3] Specific inhibitors are therefore required for further understanding of the pharmacological and physiological roles of this interesting transporter in normal and malignant stem cells, as well as of clinical applications of BCRP inhibition in cancer chemotherapy. Two BCRP inhibitors—GF120918 and fumitremorgin C (**6**)—have been well characterized. GF120918 is a synthetic product originally developed as a P-glycoprotein inhibitor.[4,5] In contrast, compound **6**, a diketopiperazine mycotoxin produced by *Aspergillus fumigatus*,[6] is capable of completely reversing mitoxantrone, doxorubicin, and topotecan resistance in BCRP-overexpressing cells but does not reverse resistance to cells that overexpress other multidrug transporters such as P-glycoprotein or multidrug-resistant protein 1.[7,8] Several synthetic analogues of **6** have been investigated and one such, Ko143, showed more potent inhibitory effects as well as lower in vivo toxicity.[9,10] This indicates that **6** may serve as a lead compound for more potent and specific BCRP inhibitors. Elucidation of the fumitremorgin biosynthetic pathway provides a strategy for new drug design.

The *A. fumigatus* genome harbors more than 20 biosynthetic gene clusters for secondary metabolites.[11] Their gene organization allows us to predict biosynthetic products that arise from the corresponding gene clusters. It has been suggested that some of the gene clusters are involved in the biosynthesis of known fungal metabolites.[12–14] The *ftm* gene cluster has also been investigated as the most probable candidate for the biosynthesis of **6** and its related compounds.[15–17] It apparently consists of nine genes (Figure 1 A). A genetic study has indicated that the dimodular nonribosomal peptide synthetase (NRPS) gene *ftmA* encodes brevianamide F synthetase.[17] Func-

[a] *Dr. N. Kato,[+] Dr. H. Suzuki,[+] H. Takagi, Dr. Y. Asami, Dr. H. Kakeya, Dr. M. Uramoto, Dr. S. Takahashi, Dr. H. Osada*
Chemical Biology Department, Advanced Science Institute, RIKEN
Wako, Saitama 351-0198 (Japan)
Fax: (+81) 48-462-4669
E-mail: hisyo@riken.jp

[b] *Dr. T. Usui*
Graduate School of Life and Environmental Sciences, University of Tsukuba
Ibaraki 305-8572 (Japan)

[c] *Dr. Y. Sugimoto*
Division of Chemotherapy, Faculty of Pharmacy, Keio University
Tokyo 105-8512 (Japan)

[d] *Dr. H. Suzuki[+]*
Present address: Organization of Advanced Science and Technology
Kobe University
Hyogo 657-8501 (Japan)

[e] *Dr. Y. Asami*
Present address: Graduate School of Pharmaceutical Sciences
The University of Tokyo
Tokyo 113-0033 (Japan)

[f] *Dr. H. Kakeya*
Present address: Division of Bioinformatics and Chemical Genomics
Graduate School of Pharmaceutical Sciences, Kyoto University
Kyoto 606-8501 (Japan)

[+] *These authors contributed equally to this work.*

Supporting information for this article is available on the WWW under http://dx.doi.org/10.1002/cbic.200800787.

WILEY InterScience © 2009 Wiley-VCH Verlag GmbH & Co. KGaA, Weinheim

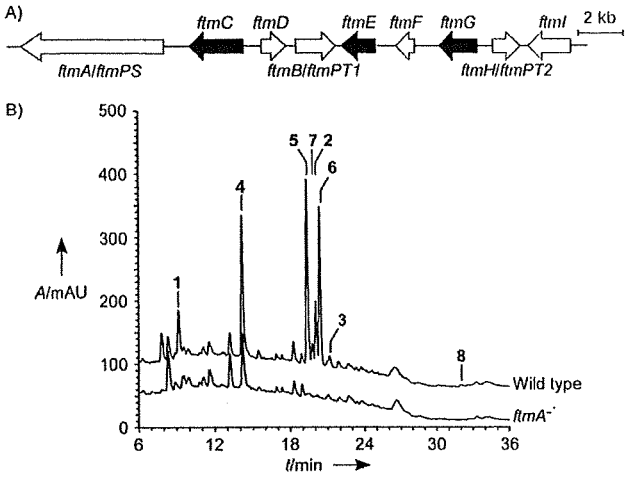

Figure 1. The production of metabolites associated with the *ftm* cluster in *A. fumigatus*. A) Gene organization of the *ftm* cluster. The three cytochrome P450 genes are indicated in black. The genes shown in gray—*ftmA/ftmPS*, *ftmB/ftmPT1*, and *ftmH/ftmPT2*—encode a dimodular NRPS[17] and prenyltransferases.[15,16] B) HPLC chromatograms of culture extracts of the wild-type and the *ftmA*⁻ strains derived from *A. fumigatus* BM939. UV detection was carried out at 220 nm. Retention times of authentic standards of fumitremorgins are denoted by Arabic numerals. MS analysis confirmed that the peak at a retention time of 14.5 min in the chromatograms of extracts of the *ftmA*⁻ strains contained no compound **4**.

tional analyses of FtmB and FtmH (also termed FtmPT1 and FtmPT2, respectively) have been performed to characterize their enzymatic activities.[15,16] These results have suggested that this gene cluster directs the biosynthesis of fumitremorgin B (**8**), with *ftmA*, *ftmB*, and *ftmH* involved in the first, second, and last steps, respectively, in the biosynthetic pathway to **8**. However, the functions of the other *ftm* genes remain to be elucidated. Lack of fumitremorgin production in the genome reference strain Af293[17] makes a full understanding of the cluster difficult, so in exploring the fumitremorgin pathway we utilized the strain BM939, which is a high producer of **6** and its related compounds.[18]

In the work reported here we carried out a structure–activity relationship (SAR) study, revealing that the most crucial event for exertion of inhibitory activity against BCRP was the C–N bond formation in the synthesis of **6**. To identify the gene responsible for the key step to form **6**, targeted gene inactivation for candidate genes in the *ftm* cluster was performed. Analysis of the knockout mutants allowed us to identify the cytochrome P450 gene *ftmE* as involved in the C–N bond formation. In addition, we demonstrated the role of the other two cytochrome P450 genes—*ftmC* and *ftmG*—in the fumitremorgin pathway.

Results and Discussion

Structure–activity relationship study based on metabolites related to the *ftm* cluster

To examine the biological activities of **6** and its related compounds, we isolated metabolites associated with the *ftm* cluster from BM939, a fumitremorgin-producing strain of *A. fumigatus*. Eight diketopiperazine compounds—brevianamide F (**1**),

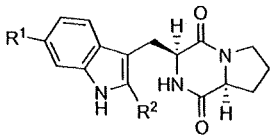

brevianamide F (**1**, R^1=H, R^2=H)
tryprostatin B (**2**, R^1=H, R^2=dimethylallyl)
desmethyltryprostatin A (**4**, R^1=OH, R^2=dimethylallyl)
tryprostatin A (**5**, R^1=OMe, R^2=dimethylallyl)

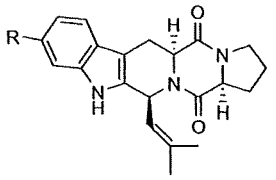

demethoxyfumitremorgin C (**3**, R=H)
fumitremorgin C (**6**, R=OMe)

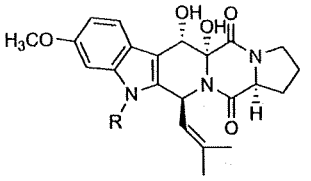

12α,13α-dihydroxyfumitremorgin C (**7**, R=H)
fumitremorgin B (**8**, R=dimethylallyl)

tryprostatin B (**2**), demethoxyfumitremorgin C (**3**), desmethyltryprostatin A (**4**), tryprostatin A (**5**), fumitremorgin C (**6**), 12α,13α-dihydroxyfumitremorgin C (**7**), and fumitremorgin B (**8**)—were prepared, and their structures were determined by mass spectrometry and NMR analysis. Compound **4**, a desmethyl analogue of **5**, is a new compound. Disruption of *ftmA* in the BM939 strain caused a deficiency in the production of **1**–**8** (Figure 1B), indicating that these metabolites are products of the *ftm* cluster

These metabolites share a diketopiperazine scaffold but are structurally diverse and thereby useful for SAR studies of their bioactivities. In fact, evaluation of **1**–**8** with regard to BCRP inhibitory activity (Figure 2A and B) revealed that **6** was the most potent inhibitor out of all of the derivatives tested. The SAR study also indicates that the following three moieties were important for the inhibitory activity of **6** against BCRP (Figure 2C). 1) The most crucial moiety involved in the activity of **6** is the covalent bond between C-3 and N-4, because compounds **3** and **6**–**8** all showed detectable activities in assays in vivo and in vitro, whereas the activities of **1**, **2**, **4**, and **5** were negligible. Although compound **5** has been reported as a BCRP inhibitor,[19] its activity was much lower than that of **6** under the conditions used in this study. 2) Dihydroxylation at C-12 and C-13 of **6** impaired inhibitory activity at the cellular level. Reversal effects of **1**–**6**, but not of **7** or **8**, on drug resist-

 © 2009 Wiley-VCH Verlag GmbH & Co. KGaA, Weinheim

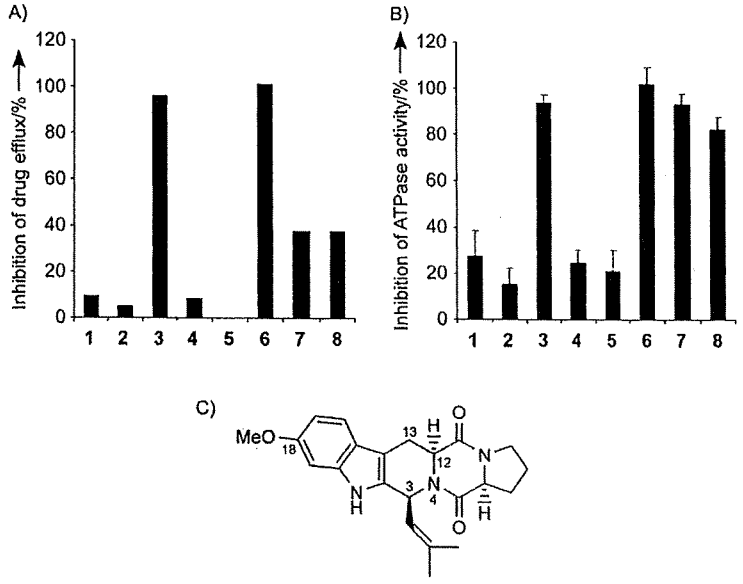

Figure 2. Evaluation of BCRP inhibitory effects of fumitremorgins. A) Inhibition of drug efflux in K562/BCRP cells by fumitremorgins **1–8**. IC_{50} values of growth inhibition of K562/BCRP cells by SN-38 in the presence of fumitremorgins (3 μM) were determined. IC_{50} values in K562/BCRP and K562 cells (parental cells) without fumitremorgins were defined as 0 and 100% inhibition, respectively. B) Inhibition of BCRP-dependent ATPase activity by fumitremorgins **1–8**. The vanadate-sensitive ATPase activities in the presence of fumitremorgins (50 μM) were measured in vitro with use of BCRP membranes (BD Biosciences). C) SAR of fumitremorgins. Of the moieties shown in gray, the covalent bond between C-3 and N-4 and the methoxy group at C-18 are important for the inhibitory activity of **6** against BCRP, whereas dihydroxylation at C-12 and C-13 of **6** affects the activity at the cellular level.

ance in BCRP-overexpressing K562 cells was in good agreement with their inhibitory activities against BCRP-dependent ATPase activities. A possible explanation for the weaker effects of **7** and **8** in the in vivo assay is a change in membrane permeability due to further modifications. 3) Compound **6** showed clear inhibitory activities even at submicromolar concentrations, whereas its demethoxy form **3** did not (data not shown), which suggests that the methoxy group at C-18 is important, in agreement with previous suggestions.[9]

Although fumitremorgins are harmful tremorgenic mycotoxins produced by *A. fumigatus* and related fungi,[6] some of the biosynthetic intermediates besides the BCRP inhibitor **6** have been shown to have interesting biological and pharmacological activities.[18,20] Recently, Jain et al. reported that **5**, which has inhibitory effects on the cell cycle[18] and microtubule assembly,[21] and its synthetic derivatives showed insignificant bioactivities.[22] Consistently with this, such inhibitory effects were not detectable in the compounds isolated in this study.

Identification of the key enzymes for fumitremorgin biosynthesis

The SAR study of fumitremorgins **1–8** revealed the important moieties involved in exertion of the BCRP inhibitory activity of **6**. From this information we tried to identify the genes involved in the formation of such important moieties. None of the enzymes catalyzing the cyclization to form **6**, the subsequent hydroxylation at C-12 and C-13 of **6**, or the hydroxylation at C-6 of the indole ring had been previously identified. To identify the genes responsible for these reactions, we first cloned the *ftm* cluster from the strain BM939. A 27 kb DNA fragment that covered the *ftm* cluster of strain BM939 was sequenced, revealing that the cluster is extremely similar to that of Af293 and consists of nine genes (see Table 1 for features of the *ftm* gene products). There were six uncharacterized genes in the *ftm* cluster. FtmC,

Table 1. Features of the *ftm* gene products of *A. fumigatus* BM939.

Protein	Size bp/aa	exon	Function[a]	Relatives[b] (identity/similarity [%])	Accession number
FtmA	6636/2211	1–6636	dimodular NRPS	nonribosomal peptide synthetase XyNRPSA from *Xylaria* sp. BCC 1067 (37/55)	ABF29402
FtmC	1955/559	1–969, 1033–1154, 1227–1525, 1597–1698, 1768–1955	cytochrome P450	isotrichodermin C-15 hydroxylase TRI11 from *Fusarium sporotrichioides* (31/46)	O13317
FtmD	1114/342	1–528, 614–1114	methyltransferase	cercosporin toxin biosynthesis protein CTB3 from *Cercospora nicotianae* (31/51)	ABC79591
FtmB	1464/464	1–1262, 1332–1464	prenyltransferase	dimethylallyltryptophan synthase DmaW from *Claviceps purpurea* (34/56)	AAP81210
FtmE	1581/526	1–1581	cytochrome P450	cytochrome P450 ELN2 from *Coprinopsis cinerea* (26/44)	BAA33717
FtmF	876/291	1–876	α-KG dioxygenase	fumonisin C-5 hydroxylase Fum3p/FUM9 from *Gibberella moniliformis* (29/48)	AAG27131
FtmG	1813/504	1–207, 273–389, 451–550, 604–672, 723–1313, 1383–1813	cytochrome P450	GA14-synthase P450-1 from *G. fujikuroi* (37/56)	CAA75565
FtmH	1349/427	1–1181, 1247–1349	prenyltransferase	tryptophan dimethylallyltransferase FgaPT2 from *A. fumigatus* (37/56)	AAX08549
FtmI	2043/680	1–2043	protein–protein interaction	ankyrin 1 isoform 2 from *Homo sapiens* (35/53)	NP_065210

[a] Functions of FtmD, FtmF, and FtmI were predicted on the basis of sequence similarities to known proteins. α-KG: α-ketoglutarate. [b] The listed homologous proteins exclude putative proteins derived from genomic projects.

 © 2009 Wiley-VCH Verlag GmbH & Co. KGaA, Weinheim

FtmE, and FtmG show similarity to cytochrome P450s of filamentous fungi, while FtmF has similarity to proteins that belong to the α-ketoglutarate dioxygenase family.[23] These enzymes could have roles in the cyclization as well as in the hydroxylations. Besides the oxygenases, FtmD is predicted to function as an *O*-methyltransferase and is thus implicated in the methylation of the new intermediate **4** to give **5**. The *ftmI* gene encodes an ankyrin-repeat protein.[24]

To assign the roles of the oxygenase genes in fumitremorgin biosynthesis, we generated gene disruptants by replacing the entire coding region of each gene with the hygromycin B-resistance gene cassette (Δ*ftm*::*hph*; Figure 3). The *akuA*$^-$ strain (TAFK1.39), derived from BM939, was used as a host strain for the knockout experiments, and correct disruption events occurred in almost all hygromycin-resistant transformants (data not shown). Two to four transformants of each *ftm* disruption were cultivated for analysis of fumitremorgin production. The metabolite profiles of the disruptants—*ftmC*$^-$, *ftmE*$^-$, *ftmF*$^-$, and *ftmG*$^-$—were determined by HPLC and LC/ESI-MS (see Table S1 in the Supporting Information for productivity of fumitremorgins in the disruptants).

The disruption of *ftmC* led to substantial accumulation of **2** and its cyclization product **3** (Figure 4A). Compound **4** (the product hydroxylated at C-6 of the indole ring of **2**) and its downstream methoxy-group-containing metabolites **5**–**8** were not detected in the culture extracts of the *ftmC*$^-$ strain. The *ftmE* disruptants produced **2** and **5** but not their cyclization products **3** and **6** (Figure 4B). The disruption of *ftmG* resulted in the loss of production of **7** and **8** (Figure 4C). The production of **6** was observed in the *ftmG*$^-$ strain, indicating that hydroxylation of the indole ring and cyclization proceeded normally in this strain. These results clearly suggest the roles of the three cytochrome P450 genes in the fumitremorgin pathway: hydroxylation at C-6 of the indole ring, C–N bond formation to form **6**, and the subsequent dihydroxylation are mediated by *ftmC*, *ftmE*, and *ftmG*, respectively. On the other hand, the disruption of *ftmF* had no significant effect on the production of **1**–**8**, suggesting that *ftmF* should not be involved in their biosynthesis (data not shown).

On the basis of the phenotypes of the *ftm* disruptants, the functions of the three cytochrome P450 genes were demonstrated by use of a yeast expression system. The cytochrome P450 genes *ftmC*, *ftmE*, and *ftmG* were expressed in *Saccharomyces cerevisiae* with a P450 reduction partner gene of *A. fumigatus*, *AFUA_2g07940*. Microsomes that were prepared from *ftmC*-expressing yeast catalyzed the hydroxylation of **2** to

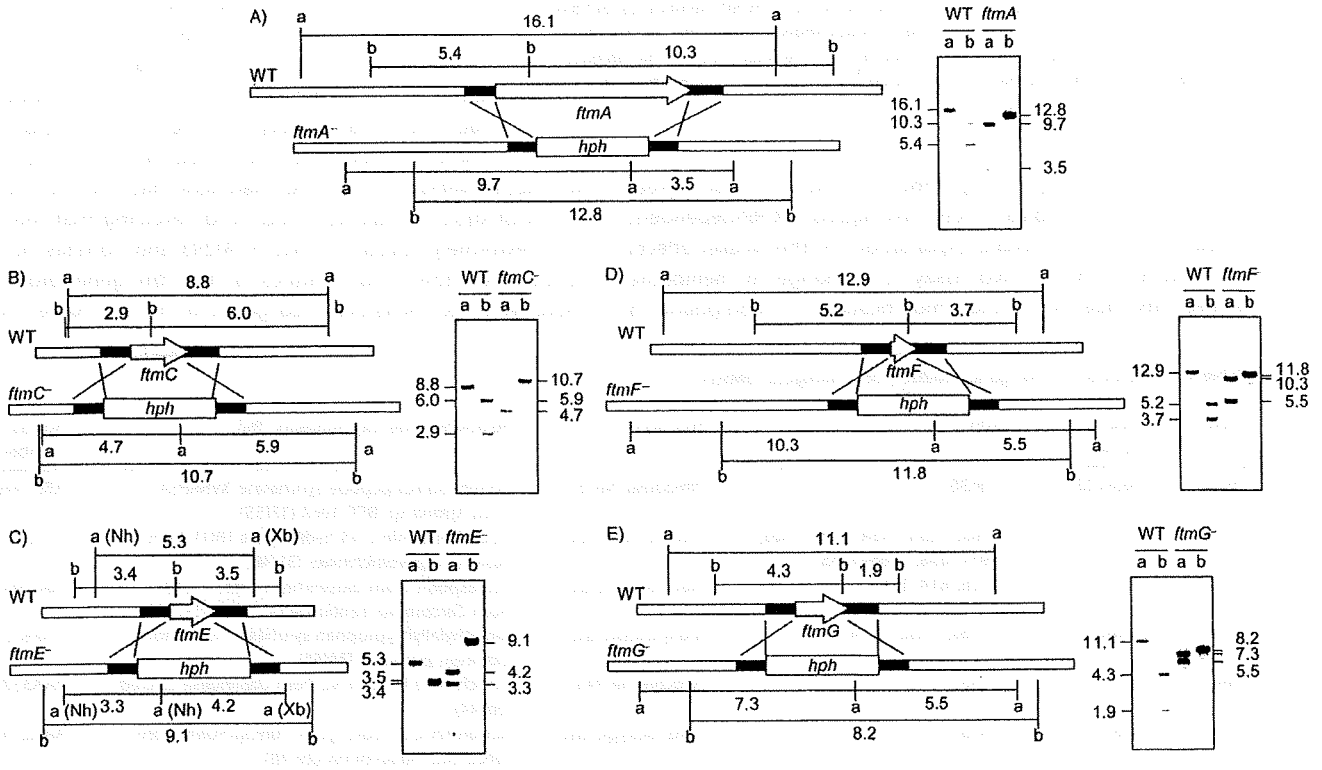

Figure 3. Construction of the *ftm* disruptants. DNA fragments (5.9 kb) containing 1 kb upstream and 1 kb downstream regions of the *ftm* genes and the hygromycin B-resistance cassette (*hph*) were used for the transformation of the wild-type strain (WT, TAFK1.39) and as probes for Southern hybridization. A) *ftmA* disruption: total DNA (10 μg) isolated from the hygromycin B-resistant transformants was digested with a) MluI, or b) ApaI. The WT strain shows a) 16.1, and b) 10.3 and 5.4 kb bands, whereas the *ftmA*$^-$ mutant shows a) 9.7 and 3.5, and b) 12.8 kb bands. B) *ftmC* disruption: total DNA was digested with a) NdeI, or b) Aor51HI. WT shows a) 8.8, and b) 6.0 and 2.9 kb bands, whereas the mutant shows a) 5.9 and 4.7, and b) 10.7 kb bands. C) *ftmE* disruption: total DNA was digested with a) NheI+XbaI, or b) KpnI. WT shows a) 5.3, and b) 3.5 and 3.4 kb bands, whereas the mutant shows a) 4.2 and 3.3, and b) 9.1 kb bands. D) *ftmF* disruption: total DNA was digested with a) NdeI, or b) NruI. WT shows a) 12.9, and b) 5.2 and 3.7 kb bands, whereas the mutant shows a) 10.3 and 5.5, and b) 11.8 kb bands. E) *ftmG* disruption: total DNA was digested with a) SacII, or b) SmaI. WT shows a) 11.1, and b) 4.3 and 1.9 kb bands, whereas the mutant shows a) 7.3 and 5.5, and b) 8.2 kb bands.

 © 2009 Wiley-VCH Verlag GmbH & Co. KGaA, Weinheim

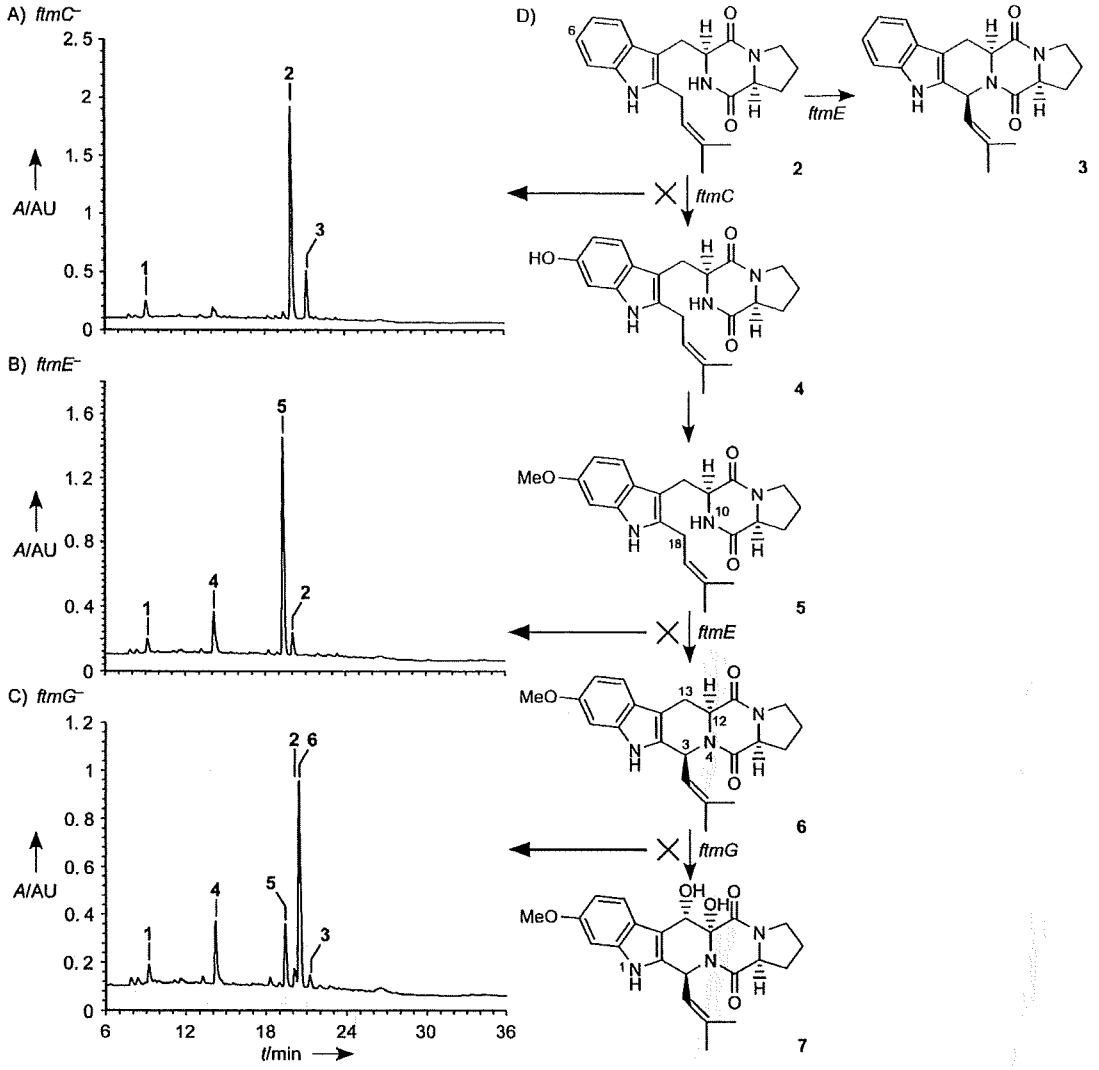

Figure 4. The metabolite profiles of the *ftm* disruptants derived from *A. fumigatus* BM939. HPLC chromatograms of culture extracts of the knockout mutants of A) *ftmC*, B) *ftmE*, and C) *ftmG*. The fungal strains were cultivated at 28 °C for 48 h. Fumitremorgins **1**–**8** in the culture extracts were determined by HPLC and LC/ESI-MS with reference to authentic standards. The production was analyzed independently in two to four clones of each strain. UV detection was carried out at 220 nm. D) Proposed biosynthetic pathway of fumitremorgins **3**–**7**.

yield **4** in the presence of NADPH (Figure 5A), even though its expression level was not high enough for the CO spectrum to be detectable. The functions of FtmE and FtmG were evaluated by bioconversion experiments: *ftmE*-expressing yeast cells converted **5** into **6** effectively (13 nM h^{-1}), whereas they also converted **2** into the shunt product **3** (6.5 nM h^{-1}; Figure 5B). Presumably these cyclizations proceeded through hydroxylation at C-18 or N-10 by FtmE, followed by dehydration to form the C–N bond. To the best of our knowledge, this is the first fungal cytochrome P450 that catalyzes C–N bond formation. Other than this, there is only one bacterial cytochrome P450, StaN, that catalyzes C–N bond formation between aglycon and deoxysugar moieties during staurosporine biosynthesis in *Streptomyces* sp. TP-A0274.[25] The conversion of **6** into **7** by *ftmG*-expressing yeast was observed, though the conversion rate was very low (4.6 nM day^{-1}; Figure 5C).

Proposed biosynthetic pathway for fumitremorgins

Previous studies have already pointed out that three genes in the *ftm* cluster—*ftmA*, *ftmB*, and *ftmH*—are involved in the first, second, and last steps, respectively, in the biosynthetic pathway of **8**.[15–17] The first committed step of the fumitremorgin pathway is the formation of **1**—diketopiperazine formation from two amino acids, L-tryptophan and L-proline. This was further supported by the lack of production of **1**–**8** that was observed in the *ftmA* disruptants derived from BM939 (Figure 1B). Heterologous expression of *ftmA* conferred the ability to produce **1** both to *S. cerevisiae* (data not shown) and to *A. nidulans*,[17] so **1** was obviously the biosynthetic product attributable to *ftmA* and was the precursor of **2**–**8**. The subsequent step is the prenylation of **1** to form **2** by FtmB/FtmPT1.[16] The other prenyltransferase, FtmH/FtmPT2, catalyzes the prenylation of the indole ring at N-1 of **7** to yield **8**.[15]

 © 2009 Wiley-VCH Verlag GmbH & Co. KGaA, Weinheim

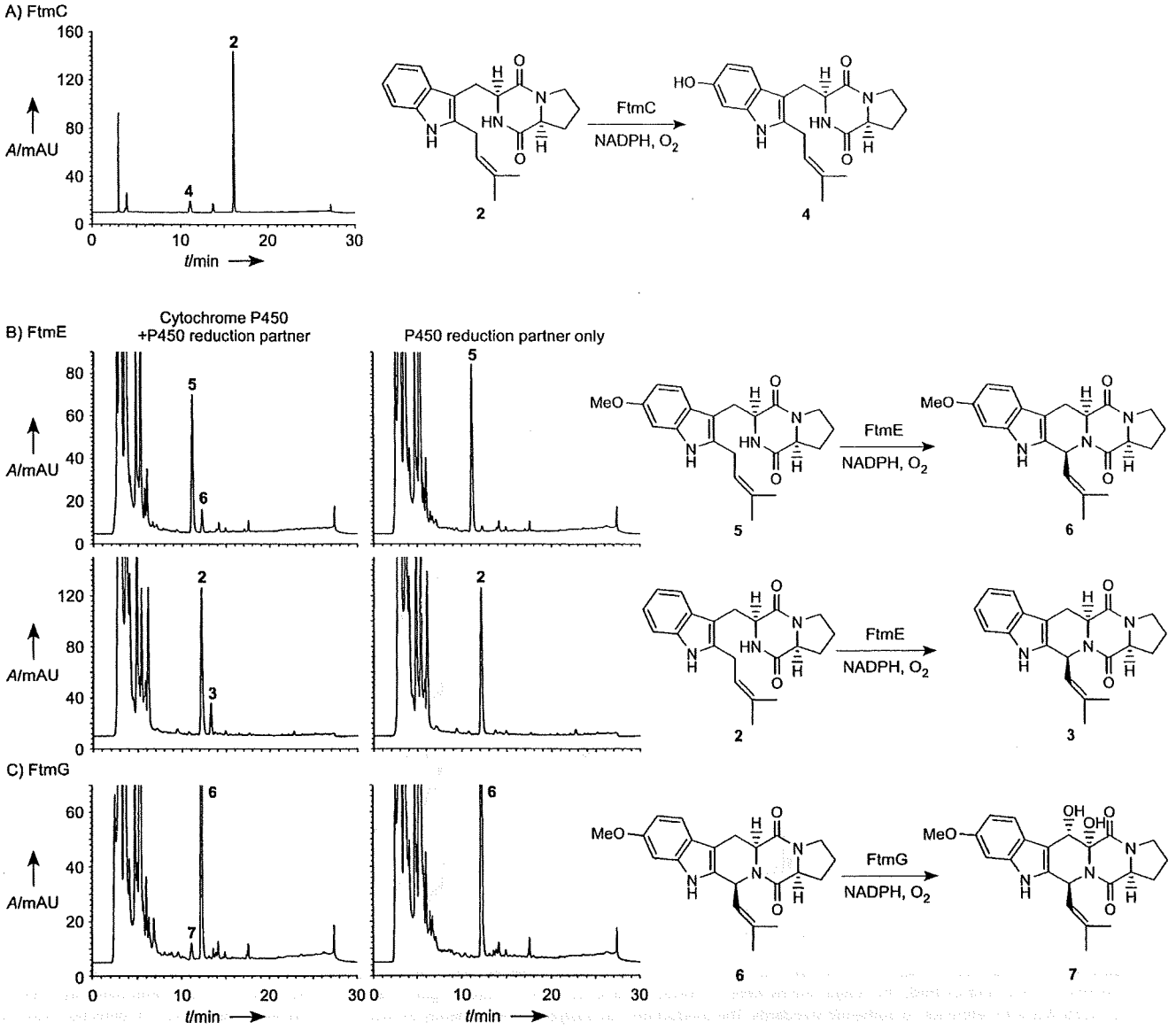

Figure 5. Reconstitution of the cytochrome P450-mediated reactions with a yeast expression system. A) HPLC chromatogram of reaction products of FtmC. Microsomes that were prepared from the yeast cells expressing *ftmC* and *AFUA_2g07940* were incubated with **2** (50 μM) in the presence of NADPH (1 mM) at 30 °C for 60 min. UV detection was carried out at 300 nm. B) HPLC chromatograms of culture extracts of the yeast cells expressing *ftmE* and *AFUA_2g07940*. The cells were incubated with substrates **5** (upper panels) and **2** (lower panels; each 2.5 μM) at 30 °C for two days. UV detection was carried out at 280 and 300 nm for reaction products of **2** and **5**, respectively. C) HPLC chromatograms of culture extracts of yeast cells expressing *ftmG* and *AFUA_2g07940*. The cells were incubated with substrate **6** (2.5 μM) at 30 °C for two days. UV detection was carried out at 300 nm.

Our results elucidated the missing link in the fumitremorgin pathway, which is composed of four processes (Figure 4 D): the hydroxylation of the indole ring of **2** at C-6 by FtmC, followed by methylation to form **5**, the C–N bond formation for the synthesis of **6** by FtmE, and the subsequent hydroxylation of **6** at C-12 and C-13 by FtmG. There are three genes—*ftmD*, *ftmF*, and *ftmI*—in the cluster that remain to be characterized. Because the predicted function of FtmD is that of a methyltransferase, FtmD is a plausible candidate for the enzyme that catalyzes the methylation of **4** to form **5**.

There are several fumitremorgin-related compounds that could not be accounted for by the *ftm* gene functions. One such compound is verruculogen, which contains a unique epidioxy (C-O-O-C) bridge in its structure.[6] To date, there is no report of enzymes that catalyze epidioxy formation except for prostaglandin endoperoxide H synthase.[26] Because the functions of three out of four oxygenase genes in the cluster—*ftmC*, *ftmE* and *ftmG*—were determined, the last uncharacterized oxygenase gene, *ftmF*, might be a candidate for this interesting reaction. FtmF-dependent peroxidation is now under investigation. The disruption of *ftmI* had no significant effect on the production of **1**–**8** (data not shown), indicating that *ftmI* was unlikely to be involved in the biosynthesis of **1**–**8**.

 © 2009 Wiley-VCH Verlag GmbH & Co. KGaA, Weinheim

Conclusions

Our SAR study on metabolites associated with the *ftm* cluster demonstrated that fumitremorgin C (**6**) was the most potent inhibitor against BCRP of all of the metabolites that were tested. A crucial moiety for exertion of the inhibitory activity of **6** was the covalent bond between C-3 and N-4. Methoxylation of the indole ring at C-6 and the dihydroxylation at C-12 and C-13 also modulated inhibitory activity. Targeted gene inactivation with a fumitremorgin producer strain, BM939, revealed that the three cytochrome P450 genes—*ftmC*, *ftmE*, and *ftmG*—are involved in these biosynthetic processes. We confirmed their enzymatic activities with a yeast expression system. In particular, the FtmE-mediated oxidative ring-closure step is noteworthy. To the best of our knowledge, this enzyme is the first fungal cytochrome P450 that catalyzes C–N bond formation. This study has elucidated the missing links in the fumitremorgin pathway, which are also crucial processes for exertion of the inhibitory activity of **6** against BCRP, not only providing insights into mycotoxin biosynthesis but also opening the way to improved biosynthesis of intermediates that have interesting pharmacological activities.

Experimental Section

Microbial strains and plasmids: *A. fumigatus* BM939 was isolated previously.[18] The cosmid AN26, which contains the hygromycin B-resistant cassette,[27] was obtained from the Fungal Genetics Stock Center. *E. coli* strains TOP10 and DH5α and plasmids pCR2.1-TOPO, pCR4Blunt-TOPO, pDONR P4-P1R/P2R-P3/221, and pDEST R4-R3 (Invitrogen) were used for DNA manipulation. *S. cerevisiae* YPH500 and pESC-URA (Stratagene) were used for heterologous expression of the *ftm* genes.

Preparation of fumitremorgins: *A. fumigatus* BM939 was cultivated at 28 °C for 3–5 days in complete medium [malt extract (2%), Bacto peptone (1%), glucose (2%)]. The fungal culture was cleared by filtration and extracted with ethyl acetate. From the dried extract, fumitremorgins were isolated by normal-phase chromatography on silica 60N (Kanto chemicals) followed by preparative HPLC. Their structures were determined from the following spectroscopic parameters.

Brevianamide F (1): ^{1}H NMR (500 MHz, $CDCl_3$): δ = 8.24 (brs, 1H), 7.57 (d, J = 7.8 Hz, 1H), 7.38 (d, J = 8.1 Hz, 1H), 7.21 (td, J = 7.3, 0.9 Hz, 1H), 7.12 (td, J = 7.3, 0.9 Hz, 1H), 7.09 (d, J = 1.8 Hz, 1H), 5.73 (brs, 1H), 4.36 (dd, J = 11.0, 2.8 Hz, 1H), 4.05 (t, J = 7.3 Hz, 1H), 3.74 (ddd, J = 15.1, 3.7, 0.9 Hz, 1H), 3.60 (m, 2H), 2.95 (dd, J = 15.1, 11.0 Hz, 1H), 2.30 (m, 1H), 1.99 (m, 2H), 1.89 ppm (m, 1H); ESI-MS: m/z: 284.1 $[M+H]^+$. The NMR spectra were identical to the reported data.[16]

Tryprostatin B (2): ^{1}H NMR (500 MHz, $CDCl_3$): δ = 7.94 (brs, 1H), 7.46 (d, J = 7.8 Hz, 1H), 7.29 (d, J = 8.3 Hz, 1H), 7.14 (ddd, J = 7.6, 7.1, 1.3 Hz, 1H), 7.08 (ddd, J = 10.6, 7.8, 1.0 Hz, 1H), 5.59 (brs, 1H), 5.30 (t, J = 7.0 Hz, 1H), 4.35 (brdd, J = 11.5, 2.8 Hz, 1H), 4.04 (t, J = 7.8 Hz, 1H), 3.64 (m, 2H), 3.57 (ddd, J = 11.8, 9.4, 3.2 Hz, 1H), 3.49 (dd, J = 17.6, 7.8 Hz, 1H), 3.44 (dd, J = 16.5, 6.9 Hz, 1H), 2.93 (dd, J = 15.1, 11.5 Hz, 1H), 2.31 (m, 1H), 2.05–2.00 (m, 2H), 1.95–1.85 (m, 1H), 1.77 (s, 3H), 1.74 ppm (s, 3H); ESI-MS: m/z: 352.1 $[M+H]^+$. The NMR spectra were identical to the reported data.[28]

Demethoxyfumitremorgin C (3): ^{1}H NMR (500 MHz, $CDCl_3$): δ = 7.79 (brs, 1H), 7.56 (d, J = 7.3 Hz, 1H), 7.33 (d, J = 8.1 Hz, 1H), 7.17 (brt, J = 6.3 Hz, 1H), 7.13 (brt, J = 6.9 Hz, 1H), 6.01 (d, J = 9.6 Hz, 1H), 4.90 (brd, J = 9.1 Hz, 1H), 4.17 (dd, J = 11.7, 5.0 Hz, 1H), 4.10 (brt, J = 8.2 Hz, 1H), 3.63 (m, 2H), 3.55 (dd, J = 16.0, 5.0 Hz, 1H), 3.11 (dd, J = 15.8, 11.5 Hz, 1H), 2.40 (m, 1H), 2.23 (m, 1H), 2.05 (m, 1H), 2.00 (s, 3H), 1.94 (m, 1H), 1.63 ppm (s, 3H); ESI-MS: m/z: 350.3 $[M+H]^+$. The NMR spectra were identical to the reported data.[26]

Desmethyltryprostatin A (4): Pale yellow powder; $[\alpha]_D^{21} = -25.5$ (c 0.25, in methanol); ^{1}H NMR (500 MHz, [D$_6$]DMSO): δ = 10.30 (s, 1H), 8.73 (s, 1H), 7.19 (d, J = 8.6 Hz, 1H), 7.03 (s, 1H), 6.62 (d, J = 2.3 Hz, 1H), 6.42 (dd, J = 2.3, 8.6 Hz, 1H), 5.27 (t, J = 7.0 Hz, 1H), 4.19 (t, J = 5.1 Hz, 1H), 3.98 (brdd, J = 7.3, 9.3 Hz, 1H), 3.45 (dd, J = 7.0, 15.5 Hz, 1H), 3.39 (m, 1H), 3.28 (dd, J = 7.0, 15.5 Hz, 1H), 3.17 (d, J = 4.5 Hz, 1H), 3.14 (dd, J = 5.1, 14.5 Hz, 1H), 2.90 (dd, J = 6.5, 14.5 Hz, 1H), 1.89 (m, 1H), 1.69 (s, 3H), 1.68 (s, 3H), 1.61 (m, 1H), 1.42 (m, 1H), 1.15 ppm (m, 1H); ^{13}C NMR (125 MHz, [D$_6$]DMSO): δ = 168.3 (s), 165.4 (s), 152.4 (s), 136.4 (s), 134.7 (s), 131.7 (s), 121.9 (d), 121.3 (s), 118.4 (d), 108.4 (d), 103.8 (s), 96.1 (d), 58.4 (d), 55.2 (d), 44.5 (t), 27.5 (t), 26.2 (t), 25.5 (q), 24.8 (t), 21.6 (t), 17.7 ppm (q); UV/Vis: λ_{max} = 222, 273, 299 nm; HR-FAB-MS: m/z: calcd for $C_{21}H_{26}N_3O_3$: 368.1974 $[M+H]^+$; found: 368.1980; ESI-MS: m/z: 368.3 $[M+H]^+$.

Tryprostatin A (5): ^{1}H NMR (500 MHz, $CDCl_3$): δ = 7.79 (brs, 1H), 7.32 (d, J = 8.7 Hz, 1H), 6.81 (d, J = 2.3 Hz, 1H), 6.74 (dd, J = 8.7, 2.3 Hz, 1H), 5.61 (brs, 1H), 5.28 (t, J = 7.3 Hz, 1H), 4.31 (brdd, J = 11.2, 2.7 Hz, 1H), 4.04 (t, J = 7.8 Hz, 1H), 3.81 (s, 3H), 3.63 (ddd, J = 10.2, 8.0, 3.7 Hz, 1H), 3.62 (dd, J = 15.1, 4.1 Hz, 1H), 3.57 (ddd, J = 11.9, 8.9, 2.8 Hz, 1H), 3.43 (dd, J = 17.4, 6.8 Hz, 1H), 3.39 (dd, J = 16.5, 7.3 Hz, 1H), 2.89 (dd, J = 15.1 11.5 Hz, 1H), 2.31 (m, 1H), 2.05–1.98 (m, 2H), 1.89 (m, 1H), 1.76 (d, J = 1.0 Hz, 3H), 1.73 ppm (s, 3H); ESI-MS: m/z: 382.3 $[M+H]^+$. The NMR spectra were identical to the reported data.[28]

Fumitremorgin C (6): ^{1}H NMR (500 MHz, $CDCl_3$): δ = 7.65 (brs, 1H), 7.42 (d, J = 8.3 Hz, 1H), 6.84 (d, J = 2.3 Hz, 1H), 6.79 (dd, J = 8.7, 2.3 Hz, 1H), 5.96 (d, J = 9.6 Hz, 1H), 4.89 (dt, J = 9.6, 1.4 Hz, 1H), 4.17 (dd, J = 11.9, 4.6 Hz, 1H), 4.09 (t, J = 7.8 Hz, 1H), 3.82 (s, 3H), 3.62 (m, 2H), 3.50 (dd, J = 16.0, 5.0 Hz, 1H), 3.08 (ddd, J = 15.8, 11.5, 0.9 Hz, 1H), 2.38 (m, 1H), 2.22 (m, 1H), 2.02 (m, 1H), 1.98 (d, J = 0.7 Hz, 3H), 1.94 (m, 1H), 1.63 ppm (d, J = 1.4 Hz, 3H); ESI-MS: m/z: 380.2 $[M+H]^+$. The NMR spectra were identical to the reported data.[28]

12α,13α-Dihydroxyfumitremorgin C (7): ^{1}H NMR (500 MHz, $CDCl_3$): δ = 7.78 (d, J = 8.7 Hz, 1H), 7.64 (brs, 1H), 6.83 (d, J = 2.3 Hz, 1H), 6.78 (dd, J = 8.7, 2.3 Hz, 1H), 5.85 (dd, J = 9.4, 0.9 Hz, 1H), 5.73 (dd, J = 2.8, 0.9 Hz, 1H), 4.78 (dt, J = 9.6, 1.4 Hz, 1H), 4.64 (d, J = 2.8 Hz, 1H), 4.41 (dd, J = 10.1, 6.9 Hz, 1H), 4.09 (brs, 1H), 3.82 (s, 3H), 3.62 (m, 2H), 2.47 (m, 1H), 2.08 (m, 1H), 2.02 (m, 1H), 1.99 (d, J = 1.4 Hz, 3H), 1.95 (m, 1H), 1.65 (d, J = 0.9 Hz, 3H); ESI-MS: m/z: 394.2 $[M+H-H_2O]^+$. The NMR spectra were identical to the reported data.[29]

Fumitremorgin B (8): ^{1}H NMR (500 MHz, $CDCl_3$): δ = 7.83 (d, J = 8.7 Hz, 1H), 6.78 (dd, J = 8.7, 2.3 Hz, 1H), 6.67 (d, J = 1.8 Hz, 1H), 5.97 (d, J = 10.1 Hz, 1H), 5.75 (s, 1H), 5.02 (brt, J = 6.9 Hz, 1H), 4.68 (brd, J = 10.1 Hz, 1H), 4.52 (brs, 2H), 4.43 (dd, J = 9.9, 7.3 Hz, 1H), 3.82 (s, 3H), 3.62 (dd, J = 8.9, 4.6 Hz, 2H), 2.46 (m, 1H), 2.20–1.90 (m, 3H), 1.97 (d, J = 1.4 Hz, 3H), 1.83 (s, 3H), 1.68 (d, J = 1.0 Hz, 3H), 1.61 (d, J = 1.4 Hz, 3H); ESI-MS: m/z: 462.1 $[M+H-H_2O]^+$. The NMR spectra were identical to the reported data.[30]

BCRP inhibitory assay: The BCRP inhibitory activities of fumitremorgins **1**–**8** were assessed by growth inhibition of K562 cells that

 © 2009 Wiley-VCH Verlag GmbH & Co. KGaA, Weinheim

overexpressed the BCRP gene (K562/BCRP) by the anticancer drug SN-38, as described previously.[31] Briefly, K562/BCRP cells were grown in RPMI 1640 medium that was supplemented with fetal bovine serum (7%, *v/v*) at 37 °C in CO_2 (5%, *v/v*). The sensitivity of the K562/BCRP cells to SN-38 in the presence of fumitremorgins (3 μM) was evaluated by cell growth inhibition after incubation at 37 °C for 4 days. Cell numbers were determined with a Coulter counter. The IC_{50} values (drug dose that caused 50% inhibition of cell growth) were determined from the growth inhibition curves.

The inhibitory effects of fumitremorgins **1**–**8** on BCRP activity were also evaluated in vitro by measuring BCRP-dependent ATPase activity, as described previously,[32] with minor modifications. BCRP membranes (BD Biosciences) were incubated at 37 °C in medium (95 μL) consisting of Tris-MES (50 mM, pH 6.8), EGTA (2 mM), DTT (2 mM), KCl (50 mM), sodium azide (5 mM), and fumitremorgins (50 μM). The ATPase reaction was started by the addition of MgATP (100 mM, 5 μL). To measure BCRP-independent ATPase activity, an identical reaction mixture that contained sodium orthovanadate (400 μM) was assayed in parallel. After incubation for 30 min, reactions were terminated by addition of perchloric acid (0.6 M, 100 μL). The amount of inorganic phosphate was determined as described previously.[33]

Cloning of the *ftm* cluster of *A. fumigatus* BM939: An AflII site was introduced into the cloning site of a cosmid vector (SuperCos1, Stratagene). The resulting vector was used for construction of a genomic library of *A. fumigatus* BM939 with AflII-digested chromosomal DNA of the strain. On screening of the library, a 27 kb cosmid clone that covered the *ftm* genes was isolated.

Disruption of the *ftm* genes: We first prepared the *akuA*-disrupted strain derived from *A. fumigatus* BM939. The *akuA* gene encodes the Ku70 component that causes low efficiency of homologous recombination in filamentous fungi.[34,35] For construction of the *akuA* knockout plasmids, 1 kb DNA fragments upstream of the start codon and downstream of the stop codon of *akuA* were amplified by PCR with use of chromosomal DNA of *A. fumigatus* BM939 as template. The primer pairs *akuA*-UF(−1023)/*akuA*-UR(−16) and *akuA*-DF(2269)/*akuA*-DR(3265) were used for amplification of the upstream and downstream regions, respectively. The pyrithiamine-resistant gene *ptrA*[36] was used as a selection marker for the *akuA* knockout. These DNA fragments were combined in the original orientation in pDEST by use of the MultiSite Gateway System (Invitrogen) in the following order: the upstream region, *ptrA*, followed by the downstream region. From this plasmid, a DNA fragment (4.0 kb) was excised by KpnI digestion and used for transformation of *A. fumigatus* BM939. Pyrithiamine-resistant transformants (Δ*akuA*::*ptrA*) that resulted from double-crossover between the disrupted *akuA* sequence and the intact chromosomal *akuA* sequence were isolated. Correct disruption was checked by Southern hybridization (data not shown). The resulting *akuA*$^-$ strain TAFK1.39 was used as a recipient strain for further transformations.

Knockout mutants of the *ftm* genes were prepared from TAFK1.39, in a procedure similar to that described for the *akuA* disruption. The 1 kb DNA fragments upstream and downstream of the *ftm* genes were amplified by PCR with use of chromosomal DNA of BM939 as template. The primer pairs *ftm*-UF and -UR and *ftm*-DF and -DR were used for amplification of the upstream and downstream regions, respectively. The hygromycin B-resistant cassette (*hph*) was used as a selection marker. These DNA fragments were combined in the original orientation in pDEST in the following order: the upstream regions, *hph*, followed by the downstream regions. From these plasmids, 5.9 kb DNA fragments were excised by restriction enzyme digestion and used for fungal transformation. The restriction enzymes that were used are indicated in Table S2. Hygromycin B-resistant transformants (Δ*ftm*::*hph*) were verified by genomic Southern analysis to contain the *ftm* gene replacements (Figure 3). Note that the parent *akuA* strain TAFK1.39 is described as the "wild-type" strain in this study. All of the DNA fragments amplified by PCR were verified by sequencing. The oligonucleotides that were used for PCR are summarized in Table S2.

Determination of fumitremorgins produced by the *ftm* disruptants: Freshly harvested spore suspensions of an *A. fumigatus* strain were inoculated in fermentation medium [K_2HPO_4 (0.5%), $MgSO_4 \cdot 7H_2O$ (0.05%), soybean meal (2%), glucose (3%), soluble starch (2%), pH 6.5]. The culture was cultivated at 28 °C for 48 h and cleared by filtration. The culture filtrate was extracted with ethyl acetate. The dried extracts were dissolved in methanol and analyzed by HPLC and LC/ESI-MS.

HPLC analysis was carried out with a Waters 600 HPLC system with a photodiode array detector (2996 PDA detector). The HPLC conditions were as follows: column, Senshu Pak Docosil-B 3 μ (4.6× 250 mm); flow rate, 1.0 mL min^{-1}; solvent A, water containing formic acid (0.05%, *v/v*); solvent B, acetonitrile. After injection of the sample into a column equilibrated with solvent B (25%), the column was developed with a linear gradient from 25% to 65% over 20 min, followed by isocratic elution of solvent B (65%) for 20 min. LC/ESI-MS analysis was carried out with a Waters Alliance HPLC system fitted with a mass spectrometer (Q-TRAP, Applied Biosystems). The HPLC conditions were as follows: column, Senshu Pak Docosil-B 3 μ (2.0×250 mm, Senshu Scientific); flow rate, 0.2 mL min^{-1}. After injection of the sample into a column equilibrated with solvent B (10%), the column was developed with a linear gradient from 10% to 100% solvent B over 90 min. Mass spectra were collected in an ESI-positive mode.

Construction of plasmids for heterologous expression of the *ftm* genes: The ORFs of *AFUA_2g07940* and *ftmE* were amplified by PCR with chromosomal DNA of *A. fumigatus* BM939 as template. The ORFs of *ftmC* and *ftmG* were amplified by two-step RT-PCR with total RNA extracted from *A. fumigatus* BM939 as template. All DNA fragments amplified by PCR were cloned into pCR4Blunt-TOPO and verified by sequencing. The *AFUA_2g07940* ORF in pCR4Blunt-TOPO was excised by SalI–XhoI digestion and cloned into the SalI-XhoI site of pESC-URA, resulting in pEUR07940. The ORFs of *ftmC*, *ftmE*, and *ftmG* were cloned in the NotI–SpeI site of pEUR079490, resulting in pEUR07940-*ftmC*, -*ftmE*, and -*ftmG*, respectively. These plasmids contained *AFUA_2g07940* and the *ftm* gene under the *GAL1* and *GAL10* promoters, respectively. The oligonucleotides that were used for PCR are summarized in Table S3.

In vitro assay of FtmC: *S. cerevisiae* YPH500 containing pEUR07940-*ftmC* was cultivated at 30 °C for three days in SGI medium [yeast nitrogen base (0.7%), galactose (2%), casamino acids (0.1%), with L-tryptophan and L-histidine (20 mg L^{-1}), L-leucine (30 mg L^{-1}), and adenine (200 mg L^{-1})]. From the harvested cells, microsomes were prepared as described previously.[37] The CO spectrum was undetectable. The reaction mixture (500 μL) consisted of Tris·HCl (50 mM, pH 7.5), glycerol (20%, *v/v*), 2-mercaptoethanol (15 mM), fumitremorgin substrate (50 μM), NADPH (1 mM), and microsomes. After the reaction mixtures had been incubated at 30 °C for 60 min, the reactions were terminated by addition of HCl (a final concentration of 0.1 M). Reaction products were extracted with ethyl acetate and analyzed by HPLC and LC/ESI-MS.

 © 2009 Wiley-VCH Verlag GmbH & Co. KGaA, Weinheim

Bioconversion assay of FtmE and FtmG: *S. cerevisiae* YPH500 carrying pEUR07940-*ftmE* or -*ftmG* was cultivated at 30 °C for 1 day in SGI medium. After fumitremorgin substrates had been added to the cultures (final concentrations of 2.5 μM), the cultures were further incubated for two days. The compounds in the broths were extracted with ethyl acetate and analyzed by HPLC and LC/ESI-MS.

The following conditions were used for HPLC analysis of the reaction products of in vitro and bioconversion assays: column, Senshu Pak Docosil-B (4.6×250 mm); flow rate, 1.0 mL min $^{-1}$. After injection of the sample into a column equilibrated with 20% solvent B, the column was initially developed isocratically for 3 min. The column was successively developed with a linear gradient 20% to 100% over 15 min, isocratic elution for 1 min, a linear gradient 100% to 20% over 1 min, followed by isocratic elution of solvent B (20%) over 10 min.

Accession numbers: The nucleotide sequence reported in this paper has been deposited to the GenBank/DDBJ/EMBL database under accession number AB436628.

Acknowledgements

We are grateful to Y. Koyama (Noda Institute for Scientific Research) for valuable discussions. We also thank S. Simizu, H. Ichimiya, and S. Kazami for evaluation of the bioactivities of the compounds, and T. Saito for advice and support. This work was supported in part by a Grant-in-Aid for Creative Scientific Research from the Ministry of Education, Culture, Sports, Science, and Technology of Japan, and by funding from the Special Postdoctoral Researchers Program of RIKEN (to N.K. and H.S.).

Keywords: *Aspergillus fumigatus* · biosynthesis · cytochrome P450 · fumitremorgins · natural products

[1] L. A. Doyle, D. D. Ross, *Oncogene* **2003**, *22*, 7340–7358.
[2] P. Krishnamurthy, J. D. Schuetz, *Annu. Rev. Pharmacol. Toxicol.* **2006**, *46*, 381–410.
[3] S. Zhou, J. D. Schuetz, K. D. Bunting, A. M. Colapietro, J. Sampath, J. J. Morris, I. Lagutina, G. C. Grosveld, M. Osawa, H. Nakauchi, B. P. Sorrentino, *Nat. Med.* **2001**, *7*, 1028–1034.
[4] M. de Bruin, K. Miyake, T. Litman, R. Robey, S. E. Bates, *Cancer Lett.* **1999**, *146*, 117–126.
[5] F. Hyafil, C. Vergely, P. Du Vignaud, T. Grand-Perret, *Cancer Res.* **1993**, *53*, 4595–4602.
[6] R. J. Cole, M. A. Schweikert in *Handbook of Secondary Fungal Metabolites, Vol. 1* (Eds.: R. J. Cole, M. A. Schweikert, B. B. Jarvis), Academic Press, San Diego, **2003**, pp. 222–232.
[7] S. K. Rabindran, H. He, M. Singh, E. Brown, K. I. Collins, T. Annable, L. M. Greenberger, *Cancer Res.* **1998**, *58*, 5850–5858.
[8] S. K. Rabindran, D. D. Ross, L. A. Doyle, W. Yang, L. M. Greenberger, *Cancer Res.* **2000**, *60*, 47–50.
[9] J. D. Allen, A. van Loevezijn, J. M. Lakhai, M. van der Valk, O. van Tellingen, G. Reid, J. H. Schellens, G. J. Koomen, A. H. Schinkel, *Mol. Cancer Ther.* **2002**, *1*, 417–425.
[10] A. van Loevezijn, J. D. Allen, A. H. Schinkel, G. J. Koomen, *Bioorg. Med. Chem. Lett.* **2001**, *11*, 29–32.
[11] W. C. Nierman, A. Pain, M. J. Anderson, J. R. Wortman, H. S. Kim, J. Arroyo, M. Berriman, K. Abe, D. B. Archer, C. Bermejo, J. Bennett, P. Bowyer, D. Chen, M. Collins, R. Coulsen, R. Davies, P. S. Dyer, M. Farman, N. Fedorova, N. Fedorova, T. V. Feldblyum, R. Fischer, N. Fosker, A. Fraser, J. L. Garcia, M. J. Garcia, A. Goble, G. H. Goldman, K. Gomi, S. Griffith-Jones, R. Gwilliam, B. Haas, H. Haas, D. Harris, H. Horiuchi, J. Huang, S. Humphray, J. Jimenez, N. Keller, H. Khouri, K. Kitamoto, T. Kobayashi, S. Konzack, R. Kulkarni, T. Kumagai, A. Lafon, J. P. Latge, W. Li, A. Lord, C. Lu, W. H. Majoros, G. S. May, B. L. Miller, Y. Mohamoud, M. Molina, M. Monod, I. Mouyna, S. Mulligan, L. Murphy, S. O'Neil, I. Paulsen, M. A. Penalva, M. Pertea, C. Price, B. L. Pritchard, M. A. Quail, E. Rabbinowitsch, N. Rawlins, M. A. Rajandream, U. Reichard, H. Renauld, G. D. Robson, S. Rodriguez de Cordoba, J. M. Rodriguez-Pena, C. M. Ronning, S. Rutter, S. L. Salzberg, M. Sanchez, J. C. Sanchez-Ferrero, D. Saunders, K. Seeger, R. Squares, S. Squares, M. Takeuchi, F. Tekaia, G. Turner, C. R. Vazquez de Aldana, J. Weidman, O. White, J. Woodward, J. H. Yu, C. Fraser, J. E. Galagan, K. Asai, M. Machida, N. Hall, B. Barrell, D. W. Denning, *Nature* **2005**, *438*, 1151–1156.
[12] D. M. Gardiner, B. J. Howlett, *FEMS Microbiol. Lett.* **2005**, *248*, 241–248.
[13] S. Maiya, A. Grundmann, X. Li, S. M. Li, G. Turner, *ChemBioChem* **2007**, *8*, 1736–1743.
[14] I. A. Unsold, S. M. Li, *Microbiology* **2005**, *151*, 1499–1505.
[15] A. Grundmann, T. Kuznetsova, S. S. Afiyatullov, S. M. Li, *ChemBioChem* **2008**, *9*, 2059–2063.
[16] A. Grundmann, S. M. Li, *Microbiology* **2005**, *151*, 2199–2207.
[17] S. Maiya, A. Grundmann, S. M. Li, G. Turner, *ChemBioChem* **2006**, *7*, 1062–1069.
[18] C. B. Cui, H. Kakeya, G. Okada, R. Onose, H. Osada, *J. Antibiot.* **1996**, *49*, 527–533.
[19] H. Woehlecke, H. Osada, A. Herrmann, H. Lage, *Int. J. Cancer* **2003**, *107*, 721–728.
[20] L. Wang, K. Sasai, T. Akagi, S. Tanaka, *Biochem. Biophys. Res. Commun.* **2008**, *373*, 392–396.
[21] T. Usui, M. Kondoh, C. B. Cui, T. Mayumi, H. Osada, *Biochem. J.* **1998**, *333*, 543–548.
[22] H. D. Jain, C. Zhang, S. Zhou, H. Zhou, J. Ma, X. Liu, X. Liao, A. M. Deveau, C. M. Dieckhaus, M. A. Johnson, K. S. Smith, T. L. Macdonald, H. Kakeya, H. Osada, J. M. Cook, *Bioorg. Med. Chem.* **2008**, *16*, 4626–4651.
[23] E. De Carolis, V. De Luca, *Phytochemistry* **1994**, *36*, 1093–1107.
[24] S. G. Sedgwick, S. J. Smerdon, *Trends Biochem. Sci.* **1999**, *24*, 311–316.
[25] H. Onaka, S. Asamizu, Y. Igarashi, R. Yoshida, T. Furumai, *Biosci. Biotechnol. Biochem.* **2005**, *69*, 1753–1759.
[26] W. L. Smith, R. M. Garavito, D. L. DeWitt, *J. Biol. Chem.* **1996**, *271*, 33157–33160.
[27] P. J. Punt, R. P. Oliver, M. A. Dingemanse, P. H. Pouwels, C. A. van den Hondel, *Gene* **1987**, *56*, 117–124.
[28] C. B. Cui, H. Kakeya, H. Osada, *J. Antibiot.* **1996**, *49*, 534–540.
[29] W.-R. Abraham, H.-A. Arfmann, *Phytochemistry* **1990**, *29*, 1025–1026.
[30] S. Kodato, M. Nakagawa, M. Hongu, T. Kawate, T. Hino, *Tetrahedron* **1988**, *44*, 359–377.
[31] K. Katayama, K. Masuyama, S. Yoshioka, H. Hasegawa, J. Mitsuhashi, Y. Sugimoto, *Cancer Chemother. Pharmacol.* **2007**, *60*, 789–797.
[32] B. Sarkadi, E. M. Price, R. C. Boucher, U. A. Germann, G. A. Scarborough, *J. Biol. Chem.* **1992**, *267*, 4854–4858.
[33] J. Nakazawa, J. Yajima, T. Usui, M. Ueki, A. Takatsuki, M. Imoto, Y. Y. Toyoshima, H. Osada, *Chem. Biol.* **2003**, *10*, 131–137.
[34] S. Krappmann, C. Sasse, G. H. Braus, *Eukaryotic Cell* **2006**, *5*, 212–215.
[35] Y. Ninomiya, K. Suzuki, C. Ishii, H. Inoue, *Proc. Natl. Acad. Sci. USA* **2004**, *101*, 12248–12253.
[36] T. Kubodera, N. Yamashita, A. Nishimura, *Biosci. Biotechnol. Biochem.* **2000**, *64*, 1416–1421.
[37] S. Takahashi, Y. Zhao, P. E. O'Maille, B. T. Greenhagen, J. P. Noel, R. M. Coates, J. Chappell, *J. Biol. Chem.* **2005**, *280*, 3686–3696.

Received: November 28, 2008
Published online on February 18, 2009

 © 2009 Wiley-VCH Verlag GmbH & Co. KGaA, Weinheim

Cancer Science
The official journal of the Japanese Cancer Association

Dofequidar fumarate sensitizes cancer stem-like side population cells to chemotherapeutic drugs by inhibiting ABCG2/BCRP-mediated drug export

Ryohei Katayama,[1] Sumie Koike,[1] Shigeo Sato,[1] Yoshikazu Sugimoto,[1,2] Takashi Tsuruo[1] and Naoya Fujita[1,3]

[1]Cancer Chemotherapy Center, Japanese Foundation for Cancer Research; [2]Graduate School of Pharmaceutical Sciences, Keio University, Tokyo, Japan

(Received June 15, 2009/Revised July 07, 2009/Accepted July 08, 2009/Online publication August 9, 2009)

The ATP-binding cassette (ABC) transporters (ABC-T) actively efflux structurally and mechanistically unrelated anticancer drugs from cells. As a consequence, they can confer multidrug resistance (MDR) to cancer cells. ABC-T are also reported to be phenotypic markers and functional regulators of cancer stem/initiating cells (CSC) and believed to be associated with tumor initiation, progression, and relapse. Dofequidar fumarate, an orally active quinoline compound, has been reported to overcome MDR by inhibiting ABCB1/P-gp, ABCC1/MDR-associated protein 1, or both. Phase III clinical trials suggested that dofequidar had efficacy in patients who had not received prior therapy. Here we show that dofequidar inhibits the efflux of chemotherapeutic drugs and increases the sensitivity to anticancer drugs in CSC-like side population (SP) cells isolated from various cancer cell lines. Dofequidar treatment greatly reduced the cell number in the SP fraction. Estimation of ABC-T expression revealed that ABCG2/breast cancer resistance protein (BCRP) mRNA level, but not the ABCB1/P-gp or ABCC1/MDR-associated protein 1 mRNA level, in all the tested SP cells was higher than that in non-SP cells. The *in vitro* vesicle transporter assay clarified that dofequidar had the ability to suppress ABCG2/BCRP function. Dofequidar treatment sensitized SP cells to anticancer agents *in vitro*. We compared the antitumor efficacy of irinotecan (CPT-11) alone with that of CPT-11 plus dofequidar in xenografted SP cells. Although xenografted SP tumors showed resistance to CPT-11, treatment with CPT-11 plus dofequidar greatly reduced the SP-derived tumor growth *in vivo*. Our results suggest the possibility of selective eradication of CSC by inhibiting ABCG2/BCRP. (*Cancer Sci* 2009; 100: 2060–2068)

Although conventional chemotherapy kills most tumor cells, it is believed to leave some cells behind, which might be the source of recurrence. The cells that tend to remain are thought to be cancer stem cells (CSC).[1] CSC are likely to share many properties of normal stem cells, such as a resistance to drugs and toxins through the expression of several ATP-binding cassette (ABC) transporters (ABC-T). Therefore, tumors might have a built-in population of drug-resistant pluripotent cells that can survive after chemotherapy and can repopulate the tumor.

The drug-transporting properties of some ABC-T are important markers for isolation and analysis of stem cells. Most differentiated cells accumulate the fluorescent dye Hoechst33342, but stem cells cannot accumulate the dye because of its active efflux via ABC-T. Thus, stem cells can be concentrated by collecting a population that contains only a low level of Hoechst33342 fluorescence.[2,3] These cells are referred to as side population (SP) cells. A large fraction of hematopoietic stem cells are found in the SP fraction.[4] SP cells can be isolated from many normal tissues,[3,5,6] which were enriched in lineage-specific stem cell. SP cells can be also identified in some neuroblastoma, hepatocellular carcinoma, gastrointestinal cancer, and glioblastoma cells, and in several cell lines that have been maintained in culture over long periods of time.[7–10]

By inhibiting the major transporters, tumor elimination could be achieved by reversing drug resistance. Therefore, many efforts have been devoted to developing inhibitors against ABC-T. Since the discovery of verapamil as a multidrug resistance (MDR)-reversing agent,[11] many compounds have been investigated as MDR inhibitors.[12] Most of the compounds, however, do not exhibit positive results in animal studies because of their dose-limiting toxicity.[12]

We previously reported a series of quinoline derivatives that show MDR-reversing activities in K562 cells that are resistant to doxorubicin (K562/ADM).[13] K562/ADM is a human leukemia cell line that endogenously overexpresses ABCB1/P-gp. Among these derivatives, dofequidar fumarate (dofequidar) was identified as a novel, orally active, quinoline-derivative inhibitor of ABCB1/P-gp. In preclinical studies, dofequidar reversed MDR in ABCB1/P-gp-expressing and ABCC1/MDR-associated protein (MRP) 1-expressing cancer cells *in vitro*. In addition, oral administration of dofequidar enhanced the antitumor activity of doxorubicin (ADM), vincristine, and docetaxel *in vivo*.[14–16] Thus, dofequidar is a promising MDR-reversing agent. The results of phase III clinical evaluations of dofequidar for breast cancer patients showed a relative improvement and absolute increase in response rate for patients who received dofequidar plus cyclophosphamide, doxorubicin, and fluorouracil (CAF), but the findings did not reach statistical significance. However, subgroup analysis suggested that dofequidar plus CAF therapy displayed significantly improved, progression-free survival and overall survival in patients who had not received prior therapy.[17]

Irinotecan (CPT-11) is one of the most widely prescribed drugs for many cancers.[18] It is reported that CPT-11 is exported from the cells by ABCB1/P-gp and ABCC1/MRP1.[19,20] In addition, SN-38, the active metabolite of prodrug CPT-11, is exported from the cells by ABCG2/breast cancer resistance protein (BCRP),[21] and the therapeutic efficacy of CPT-11 is strongly correlated with BCRP expression. Therefore, in the present study, we tried to evaluate the antitumor activity of dofequidar combined with CPT-11.

In the present study, we found that SP cells from various cancer cell lines exhibited MDR properties. Treatment of SP cells with dofequidar reversed the MDR phenotype by inhibiting ABCG2/BCRP. Dofequidar also reversed the drug resistance of xenografted SP cells *in vivo*. These results suggest that dofequidar may show clinical efficacy and may improve progression-free survival by inhibiting ABCG2/BCRP that is overexpressed specifically in CSC.

Material and Methods

Reagents and cell culture conditions. Fumitremorgin C (FTC) and reserpine were purchased from Alexis Corp. (Lausen,

[3]To whom correspondence should be addressed. E-mail: naoya.fujita@jfcr.or.jp

doi: 10.1111/j.1349-7006.2009.01288.x
© 2009 Japanese Cancer Association

Switzerland) and Daiichi Pharmaceutical (Tokyo, Japan), respectively. Mitoxantrone (MXR) and methotrexate (MTX) were purchased from Sigma (St. Louis, MO, USA) and Biomol International L.P. (Exeter, UK), respectively. Dofequidar and CPT-11 were kindly provided by Bayer Schering Pharma (Osaka, Japan) and Yakult Honsha Co. (Tokyo, Japan), respectively. Human cervix carcinoma HeLa cells, human epidermoid carcinoma KB-3-1 cells, and the stable transfectants of KB-3-1 cells were cultured in DMEM supplemented with 10% FBS (DMEM growth medium). Human chronic myeloid leukemia K562 and the stable transfectants, human breast cancer BSY-1, HBC-4, and HBC-5, human glioma U251, human pancreatic cancer Capan-1, human colon cancer KM12, and human stomach cancer MKN74 were cultured in RPMI-1640 medium supplemented with 10% FBS. To assess the cell viability, cells were incubated with 3-(4,5-dimethylthiazol-2-yl)-5-(3-carboxymethoxyphenyl)-2-(4-sulfophenyl)-2H-tetrazolium (MTS) (Promega, Madison, WI, USA) for 1 h and the optical density was measured using a microplate spectrophotometer (Benchmark-Plus; Bio-Rad, Richmond, CA, USA).

Analysis and SP cell sorting from various cancer cell lines using FACS Vantage. Cells were trypsinized and resuspended in ice-cold HBSS supplemented with 2% FBS at a concentration of 1×10^6 cells/mL. For SP analysis, cells were treated with 2.5–15 μg/mL Hoechst33342 dye (Invitrogen, Carlsbad, CA, USA) for 60 min at 37°C with or without ABC-T inhibitors (reserpine, FTC, or dofequidar). After washing with PBS, 3×10^4 cells were analyzed using a FACS Vantage SE flow cytometer (BD Bioscience, San Jose, CA, USA). Analysis was done using Flow Jo software (Treestar, San Carlos, CA, USA).

RNA preparation and real-time PCR. Total RNA from HeLa SP and non-SP (NSP) cells were extracted using an RNeasy Mini Kit (Qiagen, Hiden, Germany). RNA (1 μg) was reverse transcribed using SuperScript III (Invitrogen), according to the manufacturer's instructions. Then, the amount of ABCG2, ABCB1, and ABCC1 mRNA was quantified with TaqMan probes using a PCR LightCycler 480 (Roche Diagnostics, Basel, Switzerland) and normalized to the amount of GAPDH mRNA. The sequences of the primers for ABC-T are described in Table S1.

***In vivo* tumorigenicity and treatment.** Sorted HeLa SP and NSP cells were collected and resuspended in DMEM growth medium at concentrations ranging from 100 to 10 000 cells/30 μL. Cells were then mixed with 30 μL of Matrigel (BD Bioscience). This cell–Matrigel suspension was injected s.c. into 5- to 6-week-old female BALB/*c-nu/nu* (nude) mice (Charles River Laboratories, Yokohama, Japan). The mice were checked twice weekly for palpable tumor formation. The mice were then euthanized and tumors were resected and diced. A piece of tumor was sequentially injected s.c. into another 5- to 6-week-old female BALB/c nude mouse. Tumor size was measured every second day with a caliper, and tumor volumes were defined as (longest diameter) × (shortest diameter)/2.[2] When tumor size was approximately 100 mm^3, mice were sorted into four equal groups. Then, the nude mice were administered orally with dofequidar (200 mg/kg) or water as a control, 30 min before intravenous administration of CPT-11 (67 mg/kg) on days 0, 4, and 8. Bodyweight and tumor size were measured every 3 days. All animal procedures were carried out using protocols approved by the Japanese Foundation for Cancer Research Animal Care and Use Committee.

Transfection and immunoblotting. Negative control siRNA (medium GC duplex), ABCG2-1 siRNA, and ABCG2-2 siRNA were purchased from Invitrogen (Table S1). HeLa cells were transfected with various siRNA with LipofectAMINE 2000 reagent (Invitrogen), according to the manufacturer's instructions. After 24 h of incubation, cells were harvested, and the expression of ABCG2/BCRP and the cell number in the SP fraction was analyzed. For immunofluorescent staining, cells were incubated in blocking buffer (5 mg/mL of BSA and 2 mM EDTA in PBS) for 15 min. Then, 0.5 μg of biotin-conjugated anti-ABCG2/BCRP antibody (5D3; eBioscience, San Diego, CA, USA) was added. After incubation for 30 min, cells were washed and incubated with 0.1 μg of streptavidin–phycoerythrin (PE) (BD Bioscience). After washing, cells were analyzed by flow cytometry. For immunoblotting, cells were lysed in SDS sample buffer (0.1 M Tris-HCl at pH 8.0, 10% glycerol, and 1% SDS) with sonication and cleared by centrifugation at 17 400*g* for 10 min. Samples were electrophoresed and immunoblotted with the indicated antibodies: ABCG2/BCRP polyclonal antibody,[22] MDR1 antibody (JSB-1; Monosan, Uden, the Netherlands), MRP1 antibody (MRPm6, Monosan), and tubulin alpha antibody (YL1/2; Serotec, Oxford, UK).

***In vitro* vesicle transport assay.** We assayed ^{3}H-labeled MTX ([^{3}H]MTX) transport using lipid vesicles containing ABCG2/BCRP protein (Genomembrane, Yokohama, Japan), according to the manufacturer's instructions. [^{3}H]MTX was purchased from Moravek (Brea, CA, USA) (#MT701). The transport reaction (50 mM MOPS-Tris [pH 7.0], 7.5 mM $MgCl_2$, 70 mM KCl, 160 μM cold MTX, with various inhibitors [dofequidar, FTC, or verapamil], 1 mCi/mL [^{3}H]MTX, and membrane vesicles [25 μg protein]) in a 30-μL mixture was kept on ice for 5 min. Then, 20 μL of 10 mM ATP or AMP was added into reaction mixtures and incubated at 37°C for 5 min. The reaction was terminated by adding an ice-cold stop solution (40 mM MOPS-Tris [pH 7.0] and 70 mM KCl). The membrane vesicles were trapped on a TOPCOUNT plate filter and washed with ice-cold stop solution. The radioactivity was measured with a liquid scintillation counter (Topcount; Perkin Elmer, Waltham, MA, USA).

Intracellular drug accumulation. The effect of dofequidar on the intracellular accumulation of MXR was determined by flow cytometry. K562 or K562/BCRP cells (5×10^5 cells) were incubated with 3 μM MXR for 30 min at 37°C with or without dofequidar or FTC, washed in ice-cold PBS, and then subjected to fluorescence analysis using a Cytomics FC500 (Beckman Coulter, Fullerton, CA, USA) with 630 nm excitation.

Statistical analysis. All data are shown as means ± SD. Student's *t*-test was carried out. *P*-values <0.05 were considered statistically significant. All statistical tests were two sided.

Results

Identification and characterization of SP cells. Staining the cells with Hoechst33342 dye followed by flow cytometric analysis revealed the presence of a very small unstained population (i.e. the SP) of cells in primary tumors and several cell lines. SP cells are known to show cancer stem cell-like properties, such as high tumorigenicity and repopulating ability. To study the characteristics of SP cells and to develop new strategies targeting cancer stem cells, we first investigated the presence of SP cells in established human cancer cell lines. Consistent with a previous report,[10] the human cervical cancer HeLa cell line contained SP cells at approximately 0.5–1% of the total (Fig. 1A, left panels). The number of cells in the SP fraction derived from HeLa and HBC-4 cells was drastically reduced by adding the ABC-T inhibitor reserpine (Fig. 1A, right panels). Because reserpine treatment did not affect the fluorescence patterns of Hoechst33342-stained U251 glioma cells, we concluded that U251 glioma cells did not contain SP cells. However, the cell lines that contain no SP cells, like U251, might have CSC that don't overexpress ABC-T associated with Hoechst33342 efflux. We further examined the presence of SP cells in various cancer cell lines, and as shown in Figure 1(B), most cancer cell lines contained SP cells, whereas the SP fractions varied from 0.2 to 10%.

© 2009 Japanese Cancer Association

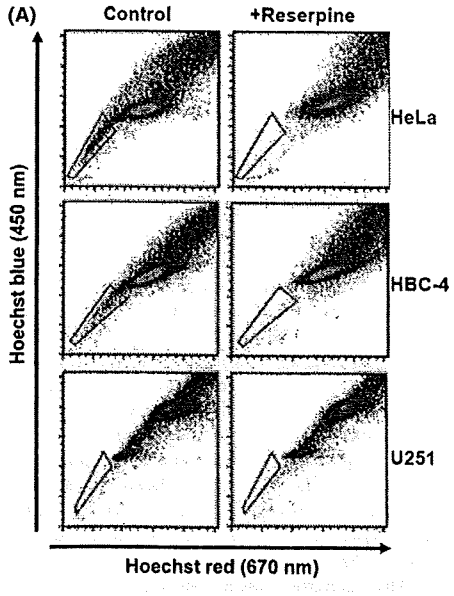

(B)

Cell lines	Tissue	SP
HeLa	Cervix	+
HBC-4	Breast	+
BSY-1	Breast	+
HBC-5	Breast	+
U251	Glioma (brain)	–
Capan-1	Pancreas	+
KM12	Colon	+
MKN74	Stomach	+

Fig. 1. The presence of side population (SP) cells in various cancer cell lines. (A) Cells were stained with Hoechst33342 in the presence (+reserpine) or absence (control) of reserpine, and were analyzed using FACS Vantage. The trapezia in each panel indicate the SP area. (B) Summary of the presence of SP cells in various human cancer cell lines. Cells were stained and the presence of SP cells examined, as described in (A). +, Presence of SP cells; –, absence of SP cells.

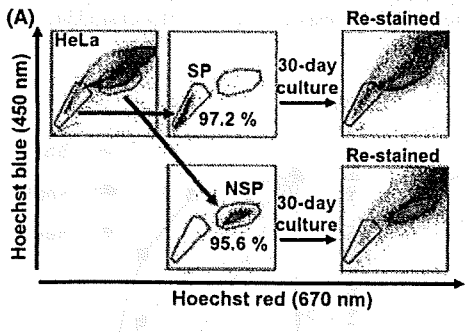

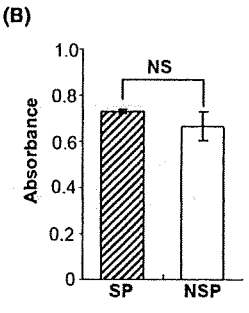

(C)

Tumor formation (HeLa, 60 days)				
Injected cell number	10^2	10^3	3×10^3	10^4
SP	6/6	6/6	6/6	5/5
NSP	6/6	6/6	6/6	6/6

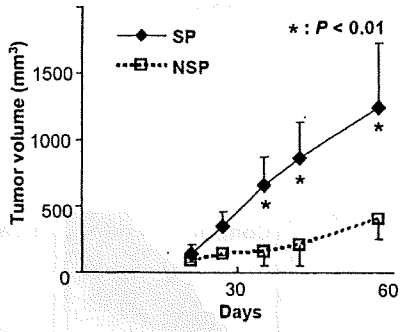

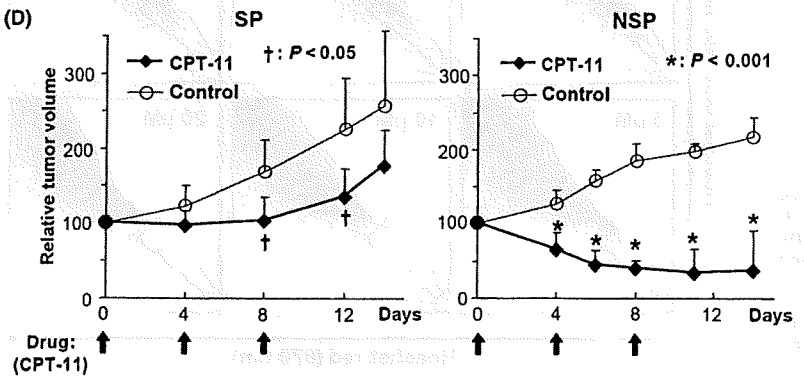

Fig. 2. Characteristics of side population (SP) cells. (A) SP and non-SP (NSP) fractions were sorted from HeLa cells. The sorting purities were confirmed by immediate reanalysis. After 30-day *in vitro* culture of the separated cells, cells were restained and analyzed (re-stained). (B) Two thousand sorted HeLa SP and NSP cells were incubated for 72 h, and the viable cell number was assessed by 3-(4,5-dimethylthiazol-2-yl)-5-(3-carboxymethoxyphenyl)-2-(4-sulfophenyl)-2H-tetrazolium (MTS) assay. No significant difference was observed between SP and NSP (NS, $P = 0.21$). (C) The indicated numbers of sorted HeLa SP and NSP cells were s.c. injected into BALB/c nude mice ($n = 6$ or 5). Tumor formation was assessed after 60 days (left). The growth of xenografts derived from one hundred sorted HeLa SP and NSP cells ($n = 6$, $^*P < 0.01$) (right). (D) The xenografted HeLa-derived SP and NSP tumors were cut into 2-mm cubes and transplanted into other mice. When secondary tumors reached approximately 100 mm^3 in volume, CPT-11 was administrated intravenously at 67 mg/kg on days 0, 4, and 8 (arrows). The graphs show the relative tumor volume ($n = 6$). ($\dagger P < 0.05$, $^*P < 0.001$).

doi: 10.1111/j.1349-7006.2009.01288.x
© 2009 Japanese Cancer Association

To examine the characteristics of SP cells, we sorted the SP and NSP cells from HeLa using a cell sorter. After sorting, SP and NSP cells were cultured in DMEM growth medium for 30 days. The cells were restained with Hoechst33342 and analyzed by flow cytometry. As shown in Figure 2(A), SP cells derived from HeLa cells showed repopulating capacity. Although NSP cells could proliferate *in vitro*, at approximately the same speed as the SP cells (Fig. 2B), the SP cell number after 30-day culture of NSP cells was smaller than that of post-culture SP cells. Thus, HeLa-derived NSP cells had weak repopulating capacity. We checked several cell lines and confirmed that the isolated SP cells could repopulate (data not shown).

We next tested the tumorigenic ability of the isolated SP cells when grafted into nude mice. When HeLa-derived SP and NSP cells were s.c. injected into nude mice, both fractions exhibited similar tumor-forming abilities (Fig. 2C, left). Interestingly, tumors derived from HeLa SP cells grew faster than those from NSP cells (Fig. 2C, right). These results suggest that HeLa SP cells, which have the ability of self-renewal and repopulation, form more aggressive tumors in nude mice than do HeLa NSP cells. To evaluate the chemoresistance of SP cells, we inoculated SP and NSP cells derived from HeLa cells. To equalize the tumor volume, the tumors that formed first were transplanted into other nude mice. The secondary tumors derived from HeLa SP cells also grew faster than those from NSP cells (data not shown). When the secondarily formed tumor volume reached 100 mm^3, the mice were treated with CPT-11. In HeLa SP-bearing mice, 4-day intervals (q4d) × 3 treatments of CPT-11 (67 mg/kg) alone arrested tumor growth without reducing the tumor volume. After termination of CPT-11 treatment, the remaining tumor started to regrow (Fig. 2D, left). However, treatment of HeLa NSP cells with q4d × 3 of 67 mg/kg of CPT-11 alone drastically reduced the tumor volume (Fig. 2D, right). These results suggest that SP-derived tumor cells had robust chemoresistance.

Dofequidar reduced the SP cell ratio. Several reports suggest that CSC show resistance to chemotherapy by expressing such ABC-T as ABCB1/P-gp and ABCG2/BCRP.[1] SP cells also have the a exporting ability of Hoechst33342, which is a substrate of ABC-T (Fig. 1). Expression of ABC-T might be associated with drug resistance in SP cells (Fig. 2D). Dofequidar (Fig. 3A) is a MDR-reversing agent currently under clinical evaluation in phase III trials.[17] Therefore, we tested the effects of dofequidar on cancer stem-like SP cells. As shown in Figure 3(B), dofequidar treatment reduced the HeLa cell number in the SP fraction dose dependently. We obtained similar results using BSY-1 and KM12 cells (Fig. 3C). These results indicate that dofequidar suppressed Hoechst33342 export by inhibiting transporters highly expressed on SP cell surfaces but not by reducing the number of SP cells themselves.

Involvement of ABCG2/BCRP, ABCB1/MDR1, and ABCC1/MRP1 in Hoechst33342 efflux. Because SP cells were separated according to the exporting activity of Hoechst33342 dye, we tried to identify the ABC-T responsible for Hoechst33342 efflux.

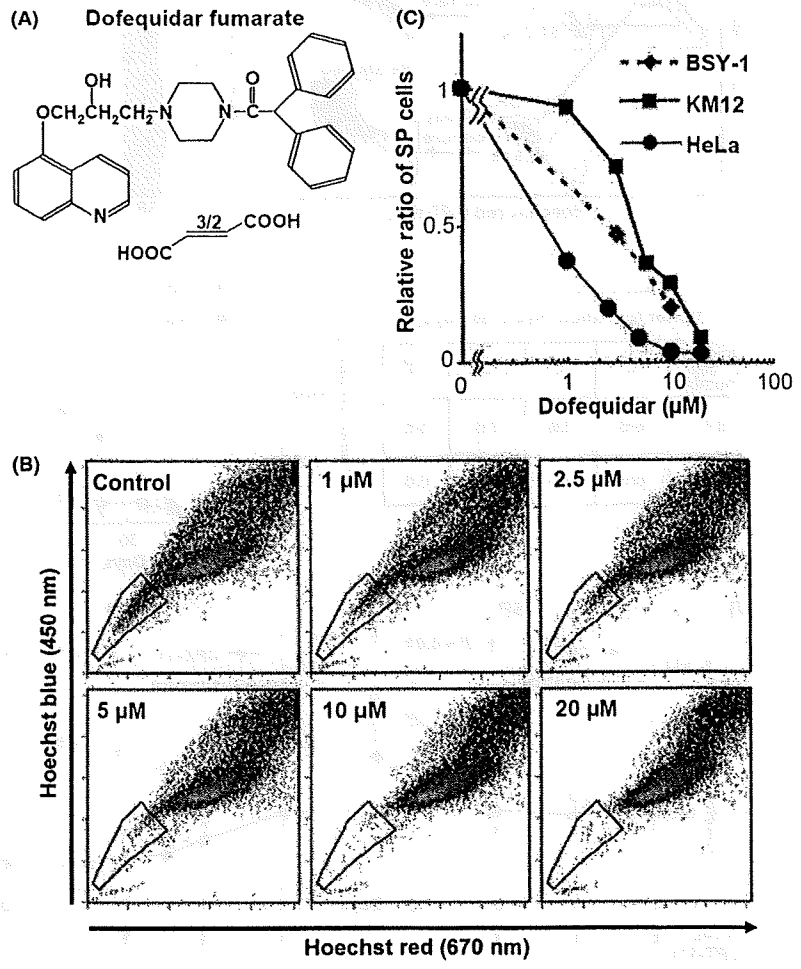

Fig. 3. Dofequidar reduced the cell number in the side population (SP) fraction. (A) Chemical structure of dofequidar. (B) HeLa cells were stained with 5 μg/mL Hoechst33342 in the presence of the indicated concentrations of dofequidar, and then analyzed. (C) Cells were stained and analyzed as in (B). The relative ratios of SP cell numbers in dofequidar-treated samples is shown by comparing with them with SP cell numbers in dofequidar-untreated samples.

© 2009 Japanese Cancer Association

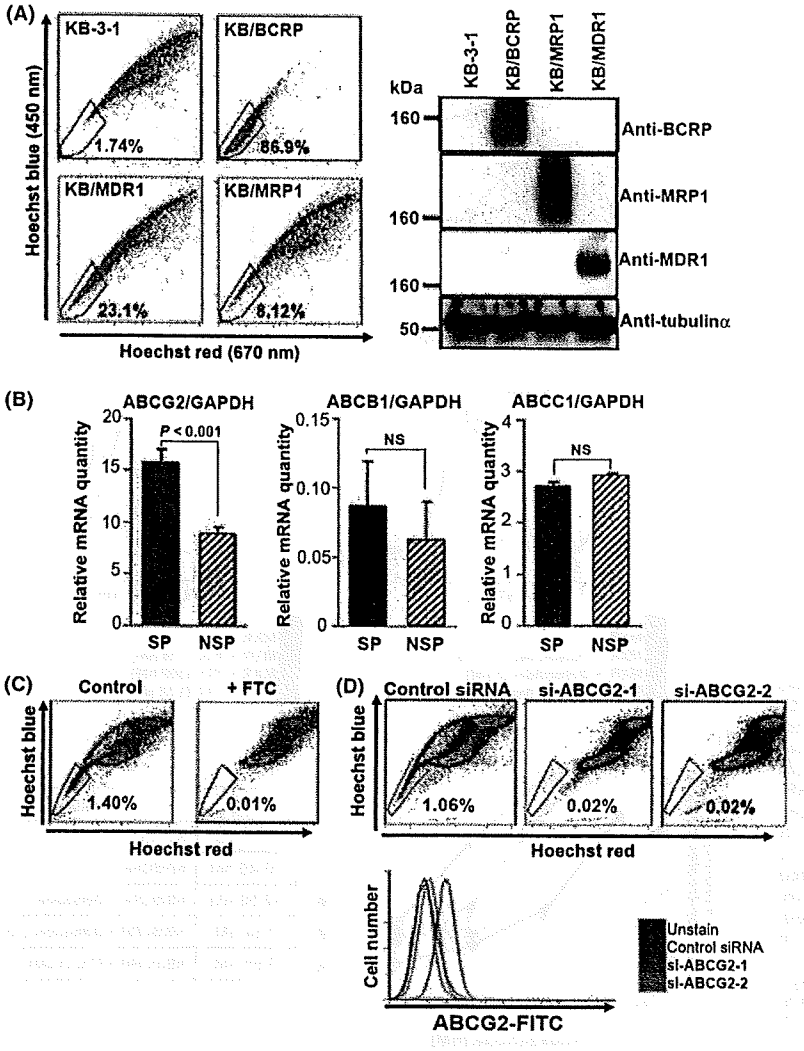

Fig. 4. Efflux of Hoechst33342 by ATP-binding cassette (ABC) G2/ABCG2/breast cancer resistance protein (BCRP), ABCB1/P-gp/multidrug resistance (MDR) 1, and ABCC1/MDR-associated protein (MRP) 1. (A) KB-3-1 and the stable transfectants were stained with Hoechst33342 and analyzed using FACS Vantage (left). The cell lysates from KB-3-1 and the stable transfectants were immunoblotted with the indicated antibodies (right). (B) mRNA was extracted from the sorted HeLa SP and NSP cells (solid and hatched columns, respectively). The graphs indicate relative mRNA expression levels of each ABC-transporter normalized with GAPDH. The expression level of ABCG2 mRNA in side population (SP) cells versus that in non-SP (NSP) cells was significantly different ($P < 0.001$). The expression levels of ABCB1 and ABCC1 mRNA were not significantly different (NS). (C) HeLa cells were stained with 5 μg/mL Hoechst33342 in the presence (+FTC) or absence (control) of 3 μM fumitremorgin C (FTC) and were analyzed. (D) HeLa cells were transfected with control siRNA or ABCG2 siRNA (si-ABCG2-1 and si-ABCG2-2). After transfection for 48 h, cells were stained with Hoechst33342 and analyzed (upper panels). The expression level of ABCG2/BCRP protein in the same samples were analyzed (lower panel).

Hoechst33342 was reported to be exported by several ABC-T, mainly ABCG2/BCRP; however, the targets of dofequidar were reported to be ABCB1/P-gp[13] and ABCC1/MRP1.[23] Then, we evaluated the Hoechst33342 export in ABCB1/P-gp-overexpressing KB-3-1 cells, ABCB1/P-gp-overexpressing KB-3-1 cells (KB/MDRI), ABCC1/MRP1-overexpressing KB-3-1 cells (KB/MRP1), and ABCG2/BCRP-overexpressing KB-3-1 cells (KB/BCRP)[22] As shown in Figure 4(A), overexpression of ABCB1/P-gp, ABCC1/MRP1, or ABCG2/BCRP in KB-3-1 cells increased the cell number in the SP fraction (23.1, 8.12, and 86.9%, respectively). Overexpression of each ABC-T did not affect the expression level of other ABC-T (Fig. 4A, right), suggesting that all of these ABC-T were associated with the Hoechst33342 efflux. We also observed that ABCG2/BCRP overexpression in K562 cells decreased Hoechst33342 blue (450 nm) fluorescence compared with parental K562 cells (Fig. S1A). We then compared the ABCB1, ABCC1, and ABCG2 mRNA expression in SP and NSP cells using a quantitative RT-PCR method. Unexpectedly, the expression levels of ABCB1 and ABCC1 mRNA were not significantly different between them. The ABCG2 mRNA expression in SP cells was significantly higher than that in NSP cells (Fig. 4B). We also observed elevated ABCG2/BCRP expression in SP cells derived from other cancer cells (data not shown). We examined the change in Hoechst33342 staining after FTC, a specific inhibitor of ABCG2/BCRP,[24] treatment, which resulted in a reduction of cell number in the SP fraction (Fig. 4C).

To further confirm the role of ABCG2/BCRP in Hoechst33342 dye efflux, we carried out Hoechst33342 staining after *ABCG2* gene silencing using two different ABCG2 siRNA. Both ABCG2 siRNA could almost completely downregulate the ABCG2/BCRP protein expression in HeLa cells (Fig. 4D, bottom panel). Under these conditions, we found a remarkable decrease in the SP cell number (Fig. 4D). These results strongly indicate that ABCG2/BCRP is mainly associated with the export of Hoechst33342 in HeLa SP cells.

Dofequidar inhibits ABCG2/BCRP in addition to ABCB1/P-gp and ABCC1/MRP1. Because dofequidar could reduce the cell number in the SP fraction that highly expressed ABCG2/BCRP (Figs 3,4), we hypothesized that dofequidar had the ability to inhibit ABCG2/BCRP in addition to the previously reported ABCB1/P-gp and ABCC1/MRP1.[13–16] Parental K562 cells or K562 stable transfectants were stained with Hoechst33342 in the presence or absence of ABC-T inhibitors. Dofequidar but not verapamil could increase the intracellular Hoechst33342 concentration in K562/BCRP cells dose dependently (Fig. S1B). We obtained similar results in KB/BCRP cells (data not shown).

doi: 10.1111/j.1349-7006.2009.01288.x
© 2009 Japanese Cancer Association

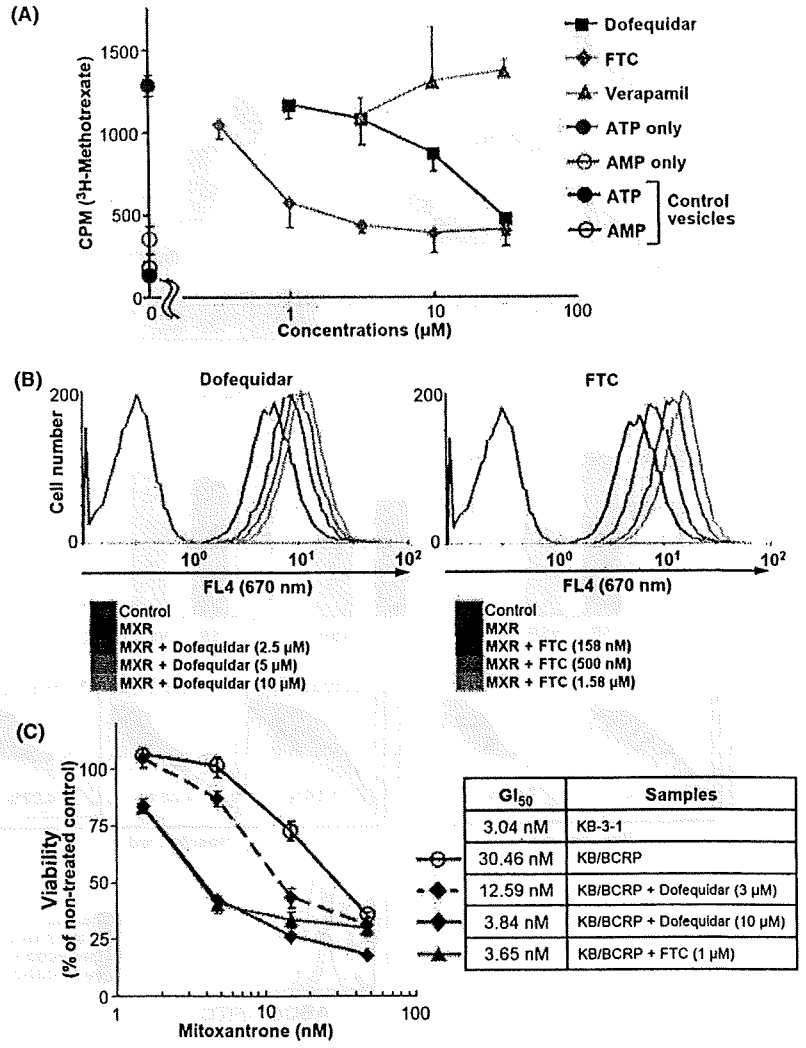

GI_{50}	Samples
3.04 nM	KB-3-1
30.46 nM	KB/BCRP
12.59 nM	KB/BCRP + Dofequidar (3 μM)
3.84 nM	KB/BCRP + Dofequidar (10 μM)
3.65 nM	KB/BCRP + FTC (1 μM)

Fig. 5. Dofequidar inhibits ATP-binding cassette (ABC) G2/ABCG2/breast cancer resistantance protein (BCRP) *in vitro* and in cells. (A) Membrane vesicles from ABCG2/BCRP-overexpressing insect cells were incubated with ^{3}H-labeled methotrexate ([^{3}H]MTX) and ATP together with vehicle (ATP only) or the indicated concentrations of dofequidar, fumitremorgin C (FTC), or verapamil at 37°C. In some experiments, membrane vesicles were incubated with [^{3}H]MTX and AMP (AMP only). Membrane vesicles from control insect cells were also incubated with [^{3}H]MTX and ATP or AMP (control vesicles). After incubation for 5 min, the incorporated [^{3}H]MTX was assayed by liquid scintillation. (B) K562/BCRP cells were incubated with 3 μM mitoxantrone (MXR) together with vehicle or the indicated concentrations of dofequidar (MXR+Dofequidar, left panel) or FTC (MXR+FTC, right panel). In some experiments, K562/BCRP cells were incubated without drugs (control). After incubation for 30 min, the fluorescence of MXR at 670 nm was analyzed. (C) KB-3-1 and KB/BCRP cells were cultured in medium containing the indicated concentration of MXR with or without dofequidar or FTC for 3 days. Cell viability was evaluated using the 3-(4,5-dimethylthiazol-2-yl)-5-(3-carboxymethoxyphenyl)-2-(4-sulfophenyl)-2H-tetrazolium (MTS) method.

To confirm the result, we carried out an *in vitro* vesicle transport assay. Membrane vesicles from control or ABCG2/BCRP-overexpressing insect cells were incubated with [^{3}H]MTX in the presence of ATP or AMP. The ATP-dependent uptake of [^{3}H]MTX was observed in ABCG2/BCRP-overexpressing membrane vesicles but not in control vesicles (Fig. 4A). FTC and dofequidar, but not verapamil, inhibited [^{3}H]MTX uptake dose dependently (Fig. 5A). These results suggest that dofequidar had the ability to inhibit ABCG2/BCRP in addition to the previously reported ABCB1/P-gp and ABCC1/MRP1.[13–16]

ABCG2/BCRP is known to export various anticancer agents, such as MTX, MXR, topotecan, and SN-38, and cause chemoresistance.[25] Accordingly, we examined whether dofequidar could reverse chemoresistance by inhibiting ABCG2/BCRP function. First, we tested whether dofequidar inhibited the export of MXR in K562/BCRP cells. K562/BCRP cells were preincubated with dofequidar or FTC for 30 min, followed by MXR incubation in the presence of inhibitors. After 30 min of incubation, MXR incorporation was analyzed by flow cytometry. As a result dofequidar inhibited MXR export, like FTC (Fig. 5B). Second, we tested whether dofequidar induced cell death in KB/BCRP cells. KB/BCRP cells showed 10-fold resistance to MXR compared to parental KB-3-1 cells. Dofequidar could sensitize the KB/BCRP in a dose-dependent fashion. Treatment with 10 μM dofequidar reversed chemoresistance, to the same level as 1 μM FTC (Fig. 5C).

Dofequidar sensitized SP cells to anticancer agents. To overcome the chemoresistance of cancer stem-like SP cells, we examined the effects of dofequidar on chemosensitivity. Although HeLa-derived SP cells showed resistance to MXR and topotecan, compared with HeLa-derived NSP cells, adding dofequidar reversed the sensitivity to MXR and topotecan to a level similar to NSP cells (Fig. 6A). To confirm the results, SP and NSP cells were separated from breast cancer BSY-1 and HBC-5 cell lines and examined for changes in chemosensitivity after dofequidar treatment. SP cells derived from BSY-1 and HBC-5 cells showed two- to four-fold resistance to chemotherapy compared with NSP cells, and dofequidar effectively sensitized SP cells and decreased the 50% growth inhibition (GI_{50}) values to a level similar to NSP cells (Fig. 6A, lower table).

FTC is not suitable for clinical studies because of its severe toxicity, but it strongly and specifically inhibits ABCG2/BCRP.[26] On the other hand, dofequidar exhibits low toxicity and has already been approved for clinical trials. To overcome the chemoresistance of cancer stem-like SP cells *in vivo*, we evaluated the antitumor activity of CPT-11 plus dofequidar in a

© 2009 Japanese Cancer Association

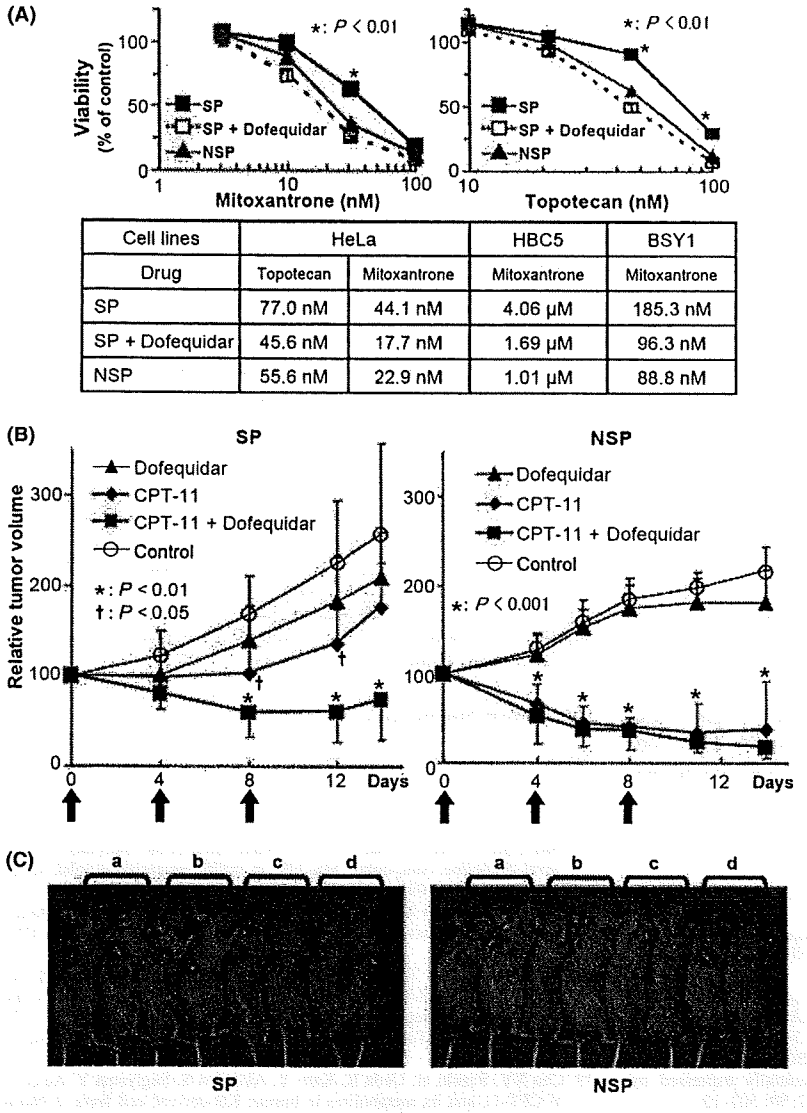

Cell lines	HeLa		HBC5	BSY1
Drug	Topotecan	Mitoxantrone	Mitoxantrone	Mitoxantrone
SP	77.0 nM	44.1 nM	4.06 μM	185.3 nM
SP + Dofequidar	45.6 nM	17.7 nM	1.69 μM	96.3 nM
NSP	55.6 nM	22.9 nM	1.01 μM	88.8 nM

Fig. 6. Sensitization by dofequidar of cancer stem-like SP cells to chemotherapeutic drugs in cells and *in vivo*. (A) SP and NSP cells from HeLa, HBC-5 or BSY-1 cells were cultured in medium containing the indicated concentration of mitoxantrone (upper left panel) or topotecan (upper right panel). In some experiments, side population (SP) cells were cultured in the presence of 3 μM dofequidar (SP+Dofequidar). The lower panel gives a summary of 50% growth inhibition (GI_{50}) values in each experiment. (B) The xenografted HeLa-derived SP and non-SP (NSP) secondary tumors were treated with 200 mg/kg dofequidar, 67 mg/kg CPT-11, or both on days 0, 4, and 8 (arrows) ($n = 6$). Graphs show relative tumor volume. The data of control and CPT-11-treated groups were the same as in Figure 2(D). The xenografted SP tumor size treated with CPT-11 versus control (†) or that treated with CPT-11 plus dofequidar versus control (*) was significantly different ($P < 0.05$ and $P < 0.01$, respectively). (C) The mice bearing HeLa SP (left) or NSP (right) tumors were photographed at 14 days after first treatment. a, Dofequidar-treated; b, CPT-11-treated; c, CPT-11 plus dofequidar-treated; d, control.

clinically relevant model. HeLa-derived SP and NSP cells were transplanted into nude mice, and the xenografted tumors were treated with CPT-11 with or without dofequidar. Dofequidar (200 mg/kg) was orally administrated 30 min before CPT-11 (67 mg/kg) injection. Although xenografted HeLa SP cells showed resistance to CPT-11, co-treatment of the mice with dofequidar drastically decreased the tumor volume (Fig. 6B, left panel), like that seen in CPT-11-treated or CPT-11 plus dofequidar-treated NSP-bearing mice (Fig. 6B, right panel). Dofequidar alone had almost no effect on SP- or NSP-derived tumor growth *in vivo*. To assess the toxicity, we measured the bodyweight of the tumor-bearing mice. The mice seemed to be healthy (Fig. 6C), and the change in bodyweight was very small (data not shown). Thus CPT-11 plus dofequidar therapy appeared to have good therapeutic efficacy *in vivo* by sensitizing cancer stem-like cells to anticancer drugs.

Discussion

It is still difficult to cure advanced cancer with chemotherapy because advanced cancer often shows resistance to many chemotherapeutic agents. Although MDR was thought to result from treatment with chemotherapy,[27] recent studies suggest that the primary tumor already has chemotherapy- or radiation therapy-resistant cells called CSC.[1] Because CSC are able to self-renew and regenerate the tumor, as likely as primary tumor, CSC are thought to be associated with recurrence. Therefore, it is important to study the characteristics of CSC and to develop new therapies targeting them.

In the present study, we used SP cells as a model of cancer stem-like cells. Various cancer cell lines contain SP cells (Fig. 1) that possess the repopulating ability (Fig. 2A). In the breast cancer cell line BSY-1, SP cells have higher cancer-initiating ability than that of NSP cells. Therefore, CSC were concentrated in BSY-1 SP cells (data not shown). On the other hand, both SP and NSP cells from the HeLa cell line could initiate tumor formation after injection of a very few number of cells (Fig. 2C). SP cells, but not NSP cells, from HeLa, however, showed resistance to several anticancer agents (Figs 2D,6A). Therefore, SP cells from cancer cell lines may not always correspond to CSC, but they may, at least, contain more malignant cells.

doi: 10.1111/j.1349-7006.2009.01288.x
© 2009 Japanese Cancer Association

To address the targeting of CSC, various efforts have been made, and several studies have reported the success of inducing cell death or differentiation in CSC.[28–32] In the present study, we showed that inhibition of ABC-T by dofequidar was one possible method to overcome anticancer drug resistance in cancer stem-like SP cells *in vitro* and *in vivo* (Figs 5,6).

In human cancer, ABCB1/P-gp, ABCC1/MRP1, and ABCG2/BCRP are the most studied, but there are more ABC-T that relate to cancer. Recently, ABCB5, originally reported to be expressed on the surface of clinically malignant melanoma and a major efflux mediator of doxorubicin in melanoma,[33] marked primitive cells (malignant melanoma-initiating cells) capable of recapitulating melanomas in xenotransplantation models. Further, targeting malignant melanoma-initiating cells with a specific antibody against ABCB5 inhibited tumor growth by inducing antibody-dependent, cell-mediated cytotoxicity.[34] Indeed, it has already been reported that some ABC-T are overexpressed in CSC.[1,7,35] Thus, it is important to understand the characteristics of ABC-T, such as its endogenous substrate, and the mechanisms of ABC-T overexpression in CSC.

From the results of phase III clinical trials of dofequidar for breast cancer patients, dofequidar treatment showed great advances in the patient group of no prior therapy.[17] This result indicates that CSC already existed in primary tumors, and they tended to remain after treatment with anticancer agents alone. Therefore, treating these patients with dofequidar plus conventional chemotherapy might effectively kill the CSC, resulting in good progression-free survival and overall survival in the clinical study. If the CSC remained, they might cause recurrence and might acquire resistance to therapy. Therefore co-administration of a MDR-reversing agent such as dofequidar in primary chemotherapy could drastically reduce the rate of recurrence.

In the present study we used CPT-11 as an anticancer agent in *in vivo* experiments (Figs 2D,6). CPT-11 is one of the most widely prescribed drugs for various cancers, including lung, stomach, colon, and cervical cancer.[18] CPT-11 is a prodrug converted into the active compound SN-38 in the liver. CPT-11 is exported from cells by ABCB1/P-gp and ABCC1/MRP1,[19,20] and the active metabolite SN-38 is exported by ABCG2/BCRP.[21] As dofequidar could inhibit ABCB1/P-gp, ABCC1/MRP1, and ABCG2/BCRP, we tried to treat xenografted tumors with CPT-11 together with dofequidar. From our study, the combination of dofequidar and CPT-11 was shown to be effective in killing of the SP cells *in vivo* without severe side effects (Fig. 6). Dofequidar could have future use as a chemotherapy-sensitizing agent targeting CSC.

Acknowledgments

We thank Drs T. Yamori, A. Tomida, and H. Seimiya for helpful discussions and Ms S. Tsukahara for technical assistance. This study was supported in part by special grants from the Ministry of Education, Culture, Sports, Science, and Technology of Japan, 19790241 and 20015046 (to R. Katayama and N. Fujita, respectively). This study was also supported in part by a grant from the Vehicle Racing Commemorative Foundation and the Mochida Memorial Foundation for Medical and Pharmaceutical Research (to N. Fujita).

Disclosure Statement

No potential conflicts of interest were disclosed.

References

1 Dean M, Fojo T, Bates S. Tumour stem cells and drug resistance. *Nat Rev* 2005; **5**: 275–84.
2 Goodell MA, Brose K, Paradis G, Conner AS, Mulligan RC. Isolation and functional properties of murine hematopoietic stem cells that are replicating *in vivo*. *J Exp Med* 1996; **183**: 1797–806.
3 Zhou S, Schuetz JD, Bunting KD *et al.* The ABC transporter Bcrp1/ABCG2 is expressed in a wide variety of stem cells and is a molecular determinant of the side-population phenotype. *Nat Med* 2001; **7**: 1028–34.
4 Scharenberg CW, Harkey MA, Torok-Storb B. The ABCG2 transporter is an efficient Hoechst 33342 efflux pump and is preferentially expressed by immature human hematopoietic progenitors. *Blood* 2002; **99**: 507–12.
5 Barile L, Messina E, Giacomello A, Marban E. Endogenous cardiac stem cells. *Prog Cardiovasc Dis* 2007; **50**: 31–48.
6 Kato K, Yoshimoto M, Kato K *et al.* Characterization of side-population cells in human normal endometrium. *Hum Reprod* 2007; **22**: 1214–23.
7 Chiba T, Kita K, Zheng YW *et al.* Side population purified from hepatocellular carcinoma cells harbors cancer stem cell-like properties. *Hepatology* 2006; **44**: 240–51.
8 Haraguchi N, Utsunomiya T, Inoue H *et al.* Characterization of a side population of cancer cells from human gastrointestinal system. *Stem Cells* 2006; **24**: 506–13.
9 Hirschmann-Jax C, Foster AE, Wulf GG *et al.* A distinct "side population" of cells with high drug efflux capacity in human tumor cells. *Proc Natl Acad Sci USA* 2004; **101**: 14 228–33.
10 Kondo T, Setoguchi T, Taga T. Persistence of a small subpopulation of cancer stem-like cells in the C6 glioma cell line. *Proc Natl Acad Sci USA* 2004; **101**: 781–6.
11 Tsuruo T, Iida H, Tsukagoshi S, Sakurai Y. Overcoming of vincristine resistance in P388 leukemia in vivo and in vitro through enhanced cytotoxicity of vincristine and vinblastine by verapamil. *Cancer Res* 1981; **41**: 1967–72.
12 Szakacs G, Paterson JK, Ludwig JA, Booth-Genthe C, Gottesman MM. Targeting multidrug resistance in cancer. *Nat Rev Drug Discov* 2006; **5**: 219–34.
13 Suzuki T, Fukazawa N, San-nohe K, Sato W, Yano O, Tsuruo T. Structure-activity relationship of newly synthesized quinoline derivatives for reversal of multidrug resistance in cancer. *J Med Chem* 1997; **40**: 2047–52.
14 Naito M, Matsuba Y, Sato S, Hirata H, Tsuruo T. MS-209, a quinoline-type reversal agent, potentiates antitumor efficacy of docetaxel in multidrug-resistant solid tumor xenograft models. *Clin Cancer Res* 2002; **8**: 582–8.
15 Nakanishi O, Baba M, Saito A *et al.* Potentiation of the antitumor activity by a novel quinoline compound, MS-209, in multidrug-resistant solid tumor cell lines. *Oncol Res* 1997; **9**: 61–9.
16 Sato W, Fukazawa N, Nakanishi O *et al.* Reversal of multidrug resistance by a novel quinoline derivative, MS-209. *Cancer Chemother Pharmacol* 1995; **35**: 271–7.
17 Saeki T, Nomizu T, Toi M *et al.* Dofequidar fumarate (MS-209) in combination with cyclophosphamide, doxorubicin, and fluorouracil for patients with advanced or recurrent breast cancer. *J Clin Oncol* 2007; **25**: 411–17.
18 Rothenberg ML. Topoisomerase I inhibitors: review and update. *Ann Oncol* 1997; **8**: 837–55.
19 Chu XY, Suzuki H, Ueda K, Kato Y, Akiyama S, Sugiyama Y. Active efflux of CPT-11 and its metabolites in human KB-derived cell lines. *J Pharmacol Exp Ther* 1999; **288**: 735–41.
20 Jansen WJ, Hulscher TM, van Ark-Otte J, Giaccone G, Pinedo HM, Boven E. CPT-11 sensitivity in relation to the expression of P170-glycoprotein and multidrug resistance-associated protein. *Br J Cancer* 1998; **77**: 359–65.
21 Kawabata S, Oka M, Shiozawa K *et al.* Breast cancer resistance protein directly confers SN-38 resistance of lung cancer cells. *Biochem Biophys Res Commun* 2001; **280**: 1216–23.
22 Kage K, Tsukahara S, Sugiyama T *et al.* Dominant-negative inhibition of breast cancer resistance protein as drug efflux pump through the inhibition of S-S dependent homodimerization. *Int J Cancer* 2002; **97**: 626–30.
23 Narasaki F, Oka M, Fukuda M *et al.* A novel quinoline derivative, MS-209, overcomes drug resistance of human lung cancer cells expressing the multidrug resistance-associated protein (MRP) gene. *Cancer Chemother Pharmacol* 1997; **40**: 425–32.
24 Rabindran SK, Ross DD, Doyle LA, Yang W, Greenberger LM. Fumitremorgin C reverses multidrug resistance in cells transfected with the breast cancer resistance protein. *Cancer Res* 2000; **60**: 47–50.
25 Mao Q, Unadkat JD. Role of the breast cancer resistance protein (ABCG2) in drug transport. *AAPS J* 2005; **7**: E118–33.
26 Allen JD, van Loevezijn A, Lakhai JM *et al.* Potent and specific inhibition of the breast cancer resistance protein multidrug transporter in vitro and in mouse intestine by a novel analogue of fumitremorgin C. *Mol Cancer Ther* 2002; **1**: 417–25.
27 Borst P, Evers R, Kool M, Wijnholds J. A family of drug transporters: the multidrug resistance-associated proteins. *J Natl Cancer Inst* 2000; **92**: 1295–302.
28 Jordan CT, Guzman ML, Noble M. Cancer stem cells. *N Engl J Med* 2006; **355**: 1253–61.

© 2009 Japanese Cancer Association

29 Ito K, Bernardi R, Morotti A *et al.* PML targeting eradicates quiescent leukaemia-initiating cells. *Nature* 2008; **453**: 1072–8.
30 Jin L, Hope KJ, Zhai Q, Smadja-Joffe F, Dick JE. Targeting of CD44 eradicates human acute myeloid leukemic stem cells. *Nat Med* 2006; **12**: 1167–74.
31 Li L, Neaves WB. Normal stem cells and cancer stem cells: the niche matters. *Cancer Res* 2006; **66**: 4553–7.
32 Piccirillo SG, Reynolds BA, Zanetti N *et al.* Bone morphogenetic proteins inhibit the tumorigenic potential of human brain tumour-initiating cells. *Nature* 2006; **444**: 761–5.
33 Frank NY, Margaryan A, Huang Y *et al.* ABCB5-mediated doxorubicin transport and chemoresistance in human malignant melanoma. *Cancer Res* 2005; **65**: 4320–33.
34 Schatton T, Murphy GF, Frank NY *et al.* Identification of cells initiating human melanomas. *Nature* 2008; **451**: 345–9.
35 Ho MM, Ng AV, Lam S, Hung JY. Side population in human lung cancer cell lines and tumors is enriched with stem-like cancer cells. *Cancer Res* 2007; **67**: 4827–33.

Supporting Information

Additional supporting information may be found in the online version of this article:

Fig. S1. Dofequidar inhibits ABCG2/BCRP in addition to ABCB1.

Table S1. Sequence information of qRT-PCR primers and siRNA for ABCG2.

Please note: Wiley-Blackwell are not responsible for the content or functionality of any supporting materials supplied by the authors. Any queries (other than missing material) should be directed to the corresponding author for the article.

doi: 10.1111/j.1349-7006.2009.01288.x
© 2009 Japanese Cancer Association